# ENERGY LOSS OF HIGH ENERGY ELECTRONS IN ALUMINUM AND COPPER.

by

James C. Goodwin

# UNITED STATES
# NAVAL POSTGRADUATE SCHOOL


# THESIS

ENERGY LOSS OF HIGH ENERGY ELECTRONS

IN ALUMINUM AND COPPER

by

James C. Goodwin, Jr.

December 1968

# ENERGY LOSS OF HIGH ENERGY ELECTRONS

# IN ALUMINUM AND COPPER

by

James C. Goodwin, Jr.
Lieutenant Commander, United States Navy
B. S., United States Naval Academy, 1958

Submitted in partial fulfillment of the
requirements for the degree of

MASTER OF SCIENCE IN PHYSICS

from the

NAVAL POSTGRADUATE SCHOOL
December 1968

ABSTRACT

The LINAC at NPGS, Monterey was used to accelerate electrons to energies ranging from 50 - 100 MeV. These were used to study energy losses of high energy electrons in aluminum and copper. The densities of each material ranged from 0.7 to 2.8 $gm/cm^2$.

The results agreed with the theory of Blunck and Westphal, unlike previous measurements made by Breuer who found disagreement between his experimental results and his interpretation of the theory of Blunck and Westphal, particularly at energies above 50 MeV and with aluminum of thickness greater than that yielding a density of 1 $gm/cm^2$.

TABLE OF CONTENTS

LIST OF TABLES

LIST OF ILLUSTRATIONS

ACKNOWLEDGMENTS

The author wishes to express his appreciation to Professor Fred R. Buskirk for his inspiration and outstanding assistance in carrying out this project, to Professor John N. Dyer for his invaluable help with both the theoretical aspects and the actual performance of the experiment, and to Professor Franz A. Bumiller who initially suggested this as a fruitful area of investigation and provided overall supervision.

The assistance of Mr. F. Ryan and 2nd Lt. L. P. Gaby in debugging computer programs is greatly appreciated. Valuable help was also given by Lt. J. W. Armstrong, Lt. N. M. Ferriter, and Lt. J. W. Stewart; members of the LINAC group.

# I. INTRODUCTION

Electrons passing through media lose energy. The principal losses are through bremsstrahlung (braking radiation), and ionization and excitation of the atomic electrons. Due to the great difference in the masses of the incident electron and the nuclei, virtually no energy is lost to recoil of the nuclei.

If a monoenergetic beam of electrons passes through a slab of matter, the transmitted electrons will emerge with energy less than the incident beam. In addition the transmitted electrons will not all lose the same amount of energy, so that a distribution of energies results. If a polyenergetic beam passes through the slab, it will already have an energy distribution when incident on the slab. By interaction with the matter, the mean of the distribution will be at a lower energy and the distribution will be broadened.

From theoretical considerations of the passage of electrons through relatively thin materials one derives a most probable energy loss, $Q_p$, and the width of the energy distribution of the exiting electrons. The width considered is the full width of the distribution at half the maximum amplitude. This will be called the "half width".

When the incident electrons scatter from the nuclei, it lengthens their path through the medium (as well as causing bremsstrahlung). For lengthening is shown to be insignificant for the energies thicknesses and media which were examined by Miller (1), who based his computations on the work of Yang (2) with data from Rossi (3). He shows that for incident energies greater than 50 MeV and absorber

thicknesses less than that yielding 5 grams of the material per square centimeter, the predicted path increases are: average path lengthening, less than 0.3%; most probable path lengthening, less than 0.2%; and maximum path lengthening for 90% of the electrons, less than 0.6%. The experimental values to be reported had incident energies greater than 53 MeV, and absorber thicknesses which yielded a maximum of 2.9 grams/$cm^2$.

Several theoretical treatments of these energy losses (4, 5, 6, 7, 8, and 9) and a few measurements (1, 10, 11, 12, and 13) are extant. Breuer (13) found agreement with the theory of Sternheimer (9) concerning most probable energy loss. He found half widths systematically larger than the values calculated by Blunck and Westphal (4).

Miller suggested that Breuer erred in his interpretation of Sternheimer when he concluded that the most probable loss due to ionization and excitation, $Q_{pi}$, varies linearly with absorber thickness. Miller also wished to examine the discrepancy between the half widths predicted by Blunck and Westphal (B & W) and those observed by Breuer.

Consequently Miller used the linear electron accelerator (LINAC) at the Naval Postgraduate School to measure the energy loss of electrons passing through aluminum, with incident energies between 60 and 100 MeV. Unfortunately many of his measurements were inconclusive due to geometrical problems encountered in the gathering of data.

Therefore these measurements were made again with a different experimental arrangement. Then a similar set of data was taken using

copper as the absorbing medium. These data (for both aluminum and copper) agree with the energy loss predictions of Blunck and Westphal.

## II. THEORY

Blunck and Westphal (B & W) (4) have developed a theoretical energy distribution for the exiting electrons which considers losses due to ionization, excitation and radiation. It is based on the works of Landau (5), Blunck and Leisegang (6), Eyges (7), and Bethe and Heitler (8). Their distribution is expressed in terms of a dimensionless parameter $\lambda$, related to the energy loss Q by:

$$\lambda = \frac{Q - \bar{Q}}{aR} + \frac{\ln E_i}{aR} - 1.116$$

$\bar{Q}$ is the average energy loss through ionization (in MeV). $E_i$ is the incident energy of the electrons (in MeV), and R is the thickness (in cm) of the absorbing medium. The constant a is a function of the atomic number Z, the atomic weight A, and the density in grams per square centimeter $\rho$ of the absorbing medium; and the velocity ($\beta = v/c$) of the electron. One finds from B & W that:

$$a = 0.154 \frac{Z}{A} \times \frac{\rho}{\beta^2} \qquad \left(\frac{\text{MeV}}{\text{cm}}\right)$$

The probability distribution W(Q)dQ is given as:

$$W(Q)dQ = B \times \left(\frac{aR}{E_i}\right)^{\alpha R} \times F_{\alpha R, b^2}(\lambda)\, d\lambda$$

and

$$F_{\alpha R, b^2}(\lambda) = \Gamma(\alpha R + 1)\left(\frac{1}{2}\right)^{\frac{\alpha R}{2}} \sum_n \frac{C_n \gamma_n e^{-\frac{(\lambda - \lambda_n)}{2(b^2 + \gamma_n^2)}}}{\sqrt{(b^2 + \gamma_n)^{1 - \alpha R}}} D_{-\alpha r}\left(-\frac{\sqrt{2}(\lambda - \lambda_n)}{\sqrt{b^2 + \gamma_n^2}}\right)$$

B is a normalizing constant. The quantities $C_n$, $\gamma_n$, $\lambda_n$ are constants given for appropriate values of the summation constant, n, in Table I below.

TABLE I. DISTRIBUTION CONSTANTS

| n | 1 | 2 | 3 | 4 |
|---|---|---|---|---|
| $C_n$ | 0.174 | 0.058 | 0.019 | 0.007 |
| $\gamma_n$ | 0.0 | 3.0 | 6.5 | 11.0 |
| $\lambda_n$ | 1.8 | 2.0 | 3.0 | 5.0 |

$\alpha$ is a constant related to the losses due to radiation. It was taken by B & W from Bethe and Heitler and is given as:

$$\alpha = 1.40 \times 10^{-3} \times \frac{Z^2}{A} \times \rho[4/3 \ln ({}^{183}/_{Z}1/3) + 1/g] \quad (\frac{1}{cm})$$

The term $b^2$ is from Blunck and Leisegang and is given by:

$$b^2 = (\frac{2}{aR}) (1.5) \sum_s \frac{I_s N_s}{Z} \times \ln\left(\frac{2E_i}{Is(1 - \beta^2)}\right)$$

where the summation is over the s different ionization potentials of the atomic electrons of the absorber. $N_s$ is the number of electrons per atom or molecule of the absorber with the ionization potential $I_s$. (When calculating $b^2$ for the copper absorbers, the ionization potentials given by Sternheimer (9(a)) were used. In this case, the factor 1.5 becomes 1.3. Another useful source of these potentials is Bearden and Burr (14).

$D_{-\alpha R}\left(-\frac{\sqrt{2}(\lambda - \lambda_n)}{\sqrt{b^2 + \gamma_n{}^2}}\right)$ is the parabolic cylinder function of the indicated arguments.

B & W calculated values of the function $F_{\alpha R,b}{}^2(\lambda)$ for 4 values of $b^2$; 0, 3, 6, and 9. These are presented graphically. Curves were drawn for $\alpha R$ values of 0, 0.05, 0.10, 0.15, 0.20, and 0.25 for each value of $b^2$. They were plotted as functions of $\lambda$, with $\lambda$ ranging from approximately -7 to +15. For a given incident energy and absorber thickness, the distribution W(Q) is directly proportional to $F_{\alpha R,b}{}^2(\lambda)$. All other terms are normalization terms. Because Q is linearly proportional to $\lambda$, one can write:

$$Q = (aR)\lambda + Q_o$$

or

$$\lambda = \frac{Q - Q_o}{aR}$$

where $Q_o$ is the energy loss corresponding to $\lambda$ equals zero, and is given by:

$$Q_o = \overline{Q} - aR \times \ln\left(\frac{E_i}{aR}\right) + 1.116(aR)$$

In evaluating $\overline{Q}$, the average energy loss due to ionization and excitation, the equations of Sternheimer (9) are used. These consider the density effect due to polarization of the medium. His equations for the average energy loss can be combined and written as:

$$\overline{Q} = \frac{A_s t}{\beta^2}\left[B_s + 0.43 + \ln E_i - \beta^2 - C - a_s\left(X_1 - \log_{10}\frac{p}{mc}\right)^{m_s}\right]$$

The terms $A_s$, $B_s$, C, $X_1$, $a_s$, and $m_s$ are constants characteristic of the absorbing material. They are found in Sternheimer 9(c) and are tabulated below for aluminum and copper.

TABLE II

| | $A_s$ | $B_s$ | C | $X_1$ | $a_s$ | $m_s$ |
|---|---|---|---|---|---|---|
| Aℓ | 0.0740 | 16.77 | -4.21 | 3 | 0.0906 | 3.51 |
| Cu | 0.0701 | 15.09 | -4.74 | 3 | 0.119 | 3.38 |

From the relativistic mass/energy relationship one can find that:

$$\frac{p}{mc} = \frac{pc}{mc^2} = \frac{\sqrt{E^2 + 2mc^2E}}{mc^2} .$$

Sternheimer (9,b) also gives an expression for the most probable energy loss due to ionization and excitation, $Q_{pi}$. Of interest is a comparison of $Q_{pi}$, the most probable loss from B & W, and experimental results. This will show the relative effects of ionization and excitation compared to that of radiation losses on the most probable energy loss. The expression for $Q_{pi}$ is:

$$Q_{pi} = \frac{A_s t}{\beta^2} \left[ B_s + 1.06 + \ln\left(\frac{A_s t}{\beta^2}\right) - \beta^2 - C - a_s \left(X_1 - \log_{10} \frac{p}{mc}\right)^{m_s} \right]$$

If one assumes a given $E_i$ and small energy losses, this expression reduces to:

$$Q_{pi} = K_1 t + K_2 t(\ln t)$$

where $K_1$ and $K_2$ are constants determined by the previous expression.

This shows the variation of the most probable energy loss (due to excitation and ionization) with absorber thickness. It is clearly non-linear in t, contrary to the interpretation of Breuer. Dividing through by t yields:

$$Q_{pi}/t = K_1 + K_2 (\ln t)$$

This shows that given an initial energy the quantity $Q_{pi}/t$ is not uniquely determined, but rather varies with the thickness of the absorber, t. Plotting $Q_{pi}/t$ versus $E_i$ results in a family of curves, each for a different absorber thickness, as shown by Miller in his figure 1; this is not a single straight line as shown by Breuer in his figure 4.

Miller shows in figure 3 a series of curves from which one can derive B & W's prediction for the values of most probable energy loss and half width. He also plots $Q_{pi}$ versus t for an $E_i$ of 70 MeV as figure 2. Figure 3 shows $Q_p$, the most probable energy loss when radiation losses are also considered, versus t for 70 MeV.

## III. EXPERIMENTAL PROCEDURE

In order to measure the energy loss of electrons passing through matter, the LINAC was used as a source of the high energy electrons. The energy of the exiting electrons was measured by using the 16 inch magnetic spectrometer described by Kenaston, Luke, and Sones (15). The energy of the incident beam was measured by using a nuclear magnetic resonance probe to measure the field of the deflection magnet of the LINAC.

If the spectrometer had been placed in a zero degree position, any beam current large enough to be stable would have saturated the counting system. For this reason, a 3.3 mil aluminum foil was placed at an angle of $45^{o}$ to the electron beam. This was used to scatter out from the main beam a secondary flux of electrons. Close behind the scattering foil were the absorbers (see figure 1). These were parallel to the beam line. The spectrometer was set at an angle of $90^{o}$ to the beam approximately 30 cm from the absorbers.

Miller's initial set-up was the same except that his absorbers were 22 cm from the scattering foil, mounted on a rotating wheel. In his "Discussion" he shows that this lead to a broadening of the energy distributions of the exiting electrons. This was due to electrons which were scattered by the absorber into the spectrometer which resulted in their appearing to have come from a displaced source with different energy. This is discussed at length by Miller. Another slight difference is that he set the spectrometer at $45^{o}$.

For this reason the absorbers were mounted close to the scattering foil (7 mm away at one end and 39 mm at the other.) In order to position absorbers of different thicknesses in place, a laminate of differing

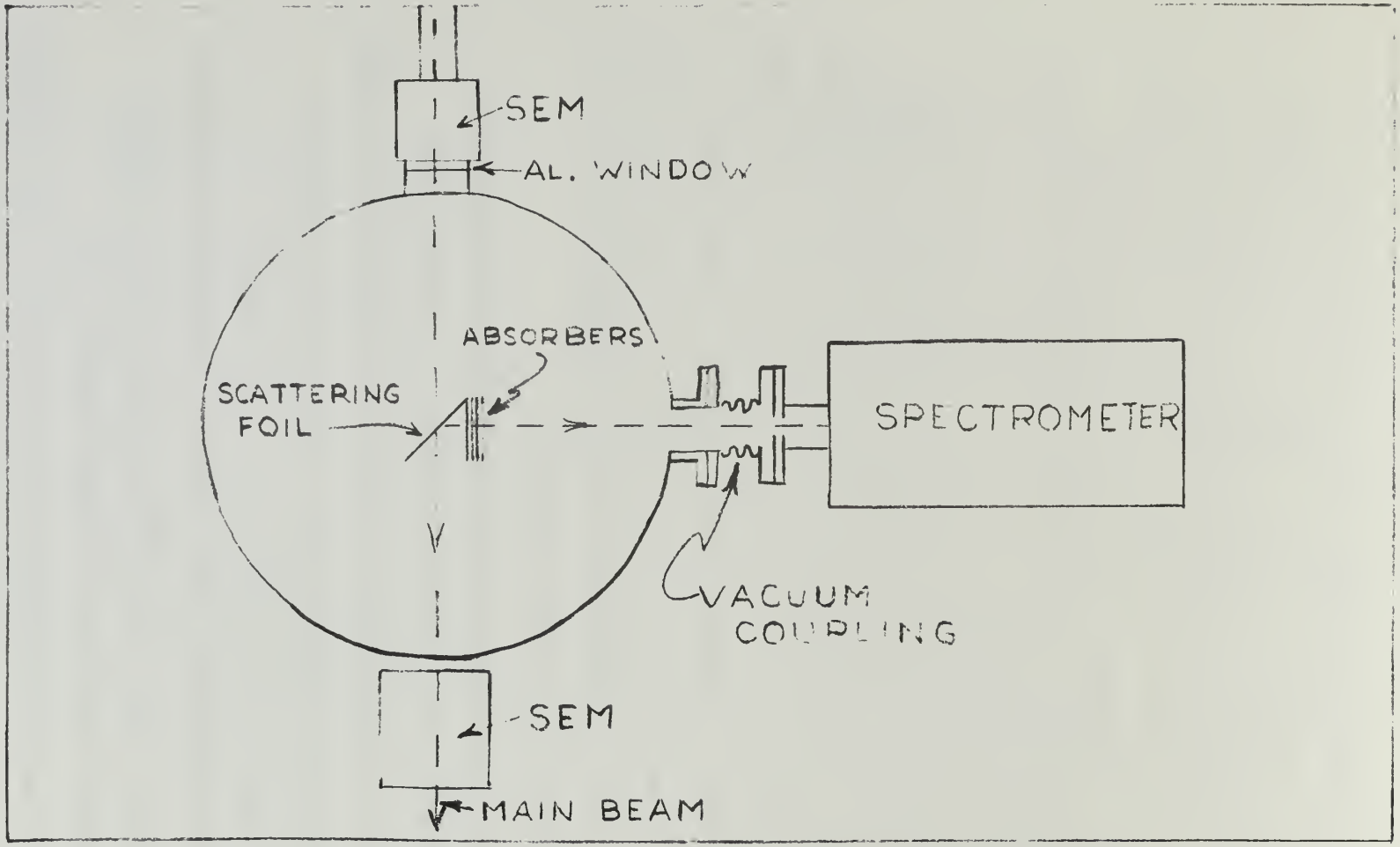


FIGURE 1. Experimental Arrangement (top view)

lengths of absorber material was raised and lowered by a piston. Figure 2 illustrates this arrangement. Because the target chamber was evacuated to approximately 50 microns there was no air between the layers of absorber material to affect the results. The absorbers were parallel to the beam and 2.2 cm away from the beam center line. They did not scatter electrons from the main beam into the spectrometer. The slot over which no scattering foil was placed was used to measure the experimental background. The topmost position which had scattering foil but no absorber behind was used to measure the energy distribution of the electrons incident on the absorbers.

The vacuum coupling described by Miller was used to couple the spectrometer to the target chamber, eliminating all windows between the absorbers and the spectrometer magnet.

The spectrometer and counting system measure the number of electrons within a small energy interval entering the magnet. For this reason many measurements at slightly different energies are necessary to construct the profile of the energy distribution. In order to ensure that each measurement represented the same amount of secondary beam incident on the absorbers a secondary emission monitor (SEM) was used to monitor the main electron beam. The output of the SEM was measured by a Cary integrating electrometer, with a 10 microfarad input capacitor. When this reached a predetermined charge counting was stopped. In this manner the data were standardized to a given amount of charge from the beam incident on the scattering foil. Typical values used are 100 millivolts to 1 volt which represent 10 to 100 microcoulombs of beam charge (because of the 10% efficiency of the SEM).

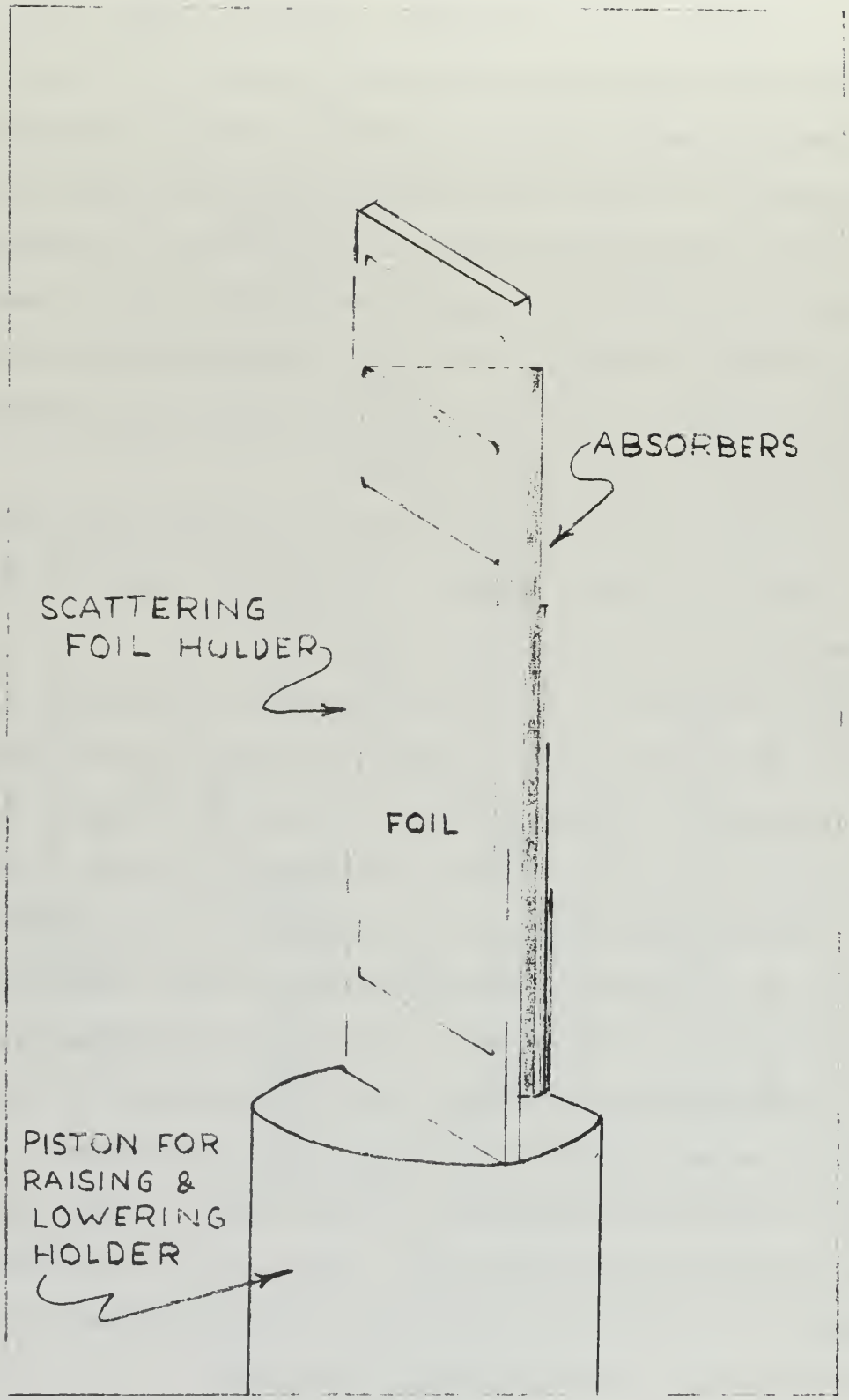


FIGURE 2. Experimental Arrangement (side view)

Data taken were: spectrometer energy setting, number of counts observed, time of integration, and voltage to which the charge on the capacitor was integrated. At approximately 1 MeV intervals the background was measured by integrating charge with the closest (to the beam) absorber in place but no scattering foil. These values were used later in determining how much background to subtract from the number of counts observed.

## IV. TREATMENT OF DATA

The theory presented earlier presumes a monoenergetic source of electrons. While the LINAC produces an essentially monoenergetic beam of electrons there is a finite width distribution in energy of the electrons comprising the beam. The secondary beam, which is incident on the absorbers, is scattered from the main beam by a thin aluminum foil and this scattering adds to the width of the energy distribution. Thus the secondary beam incident on the absorbers had an experimentally measured average half width of 0.5% of the incident energy. This width cannot be considered monoenergetic. A plot of the distribution in energy of the electrons incident on the absorbers and the resulting distributions in energy of the electrons after passing through the several absorbers is shown as figure 3. This is a plot of the values observed with incident energy 74.63 MeV and copper absorbers. It is typical of all the other combinations of energy and absorber material.

The difficulty in deriving a predicted energy loss and half width stems from the fact that neither is the incident beam monoenergetic, nor is there a simple mathematical expression for its distribution. If it were monoenergetic, the resulting distributions after passing through the absorbers could be derived from the theory presented in section II in a straightforward manner. If the beam were polyenergetic but were distributed in a simple manner, the resulting distributions could also be derived from the theory in a not so straightforward but soluble manner. One would perform the integration:

$$R(E_f) = \int_{E_i} W(E_i - E_f) \times D(E_i)\, dE_i$$

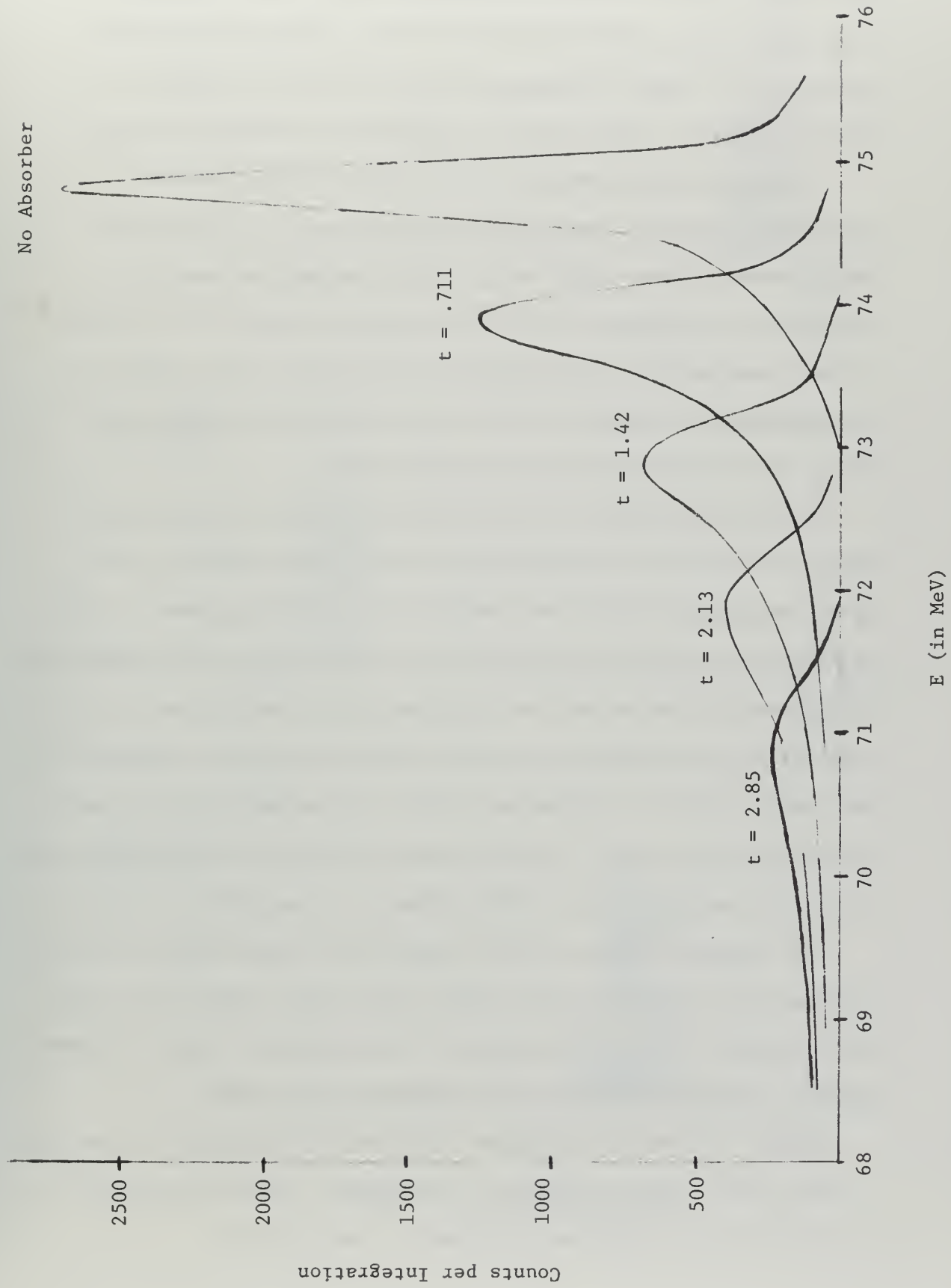


Figure 3. Energy Distribution, 74.63 MeV Incident Energy Copper Absorbers

where $R(E_f)$ is the resulting distribution, $W(E_i - E_f)$ is from the theory, and $D(E_i)$ is the hypothesized known incident distribution function. The range of integration would be over the range of incident energies. This would be a difficult integration, at best.

A very good approximation is to use the histogram method described by Miller. The incident distribution is divided into a large number of equal width energy slices and each of these is considered a monoenergetic source with amplitude given by the value of real distribution at the mid-point of the slice. The theoretical distribution was similarly divided into slices with the same width in energy as the incident beam distribution slices.

Then the amplitudes of the observed incident distribution and theory curves from B & W were fed into the IBM 360 computer at the Naval Postgraduate School and handled in the following manner. Each experimental amplitude was multiplied in turn by each of the amplitudes from the theory curves and the resulting products were stored in bins together with the appropriate energy value for that bin, determined by the theory of B & W. Succeeding products were added to the contents of the appropriate bins. In this manner resulting energy distribution predictions were generated. This process is illustrated in figure 4.

The observed values for each absorber and energy combination had previously been plotted, and a smooth curve drawn through the points. The predicted curves were normalized by the computer to have the same maximum amplitude as the faired in observed value curves.

Figure 4 shows two histograms D(E) and W(Q) being used to generate a third, R(E). They correspond to the observed initial distribution, B & W curves, and predicted distribution, respectively.

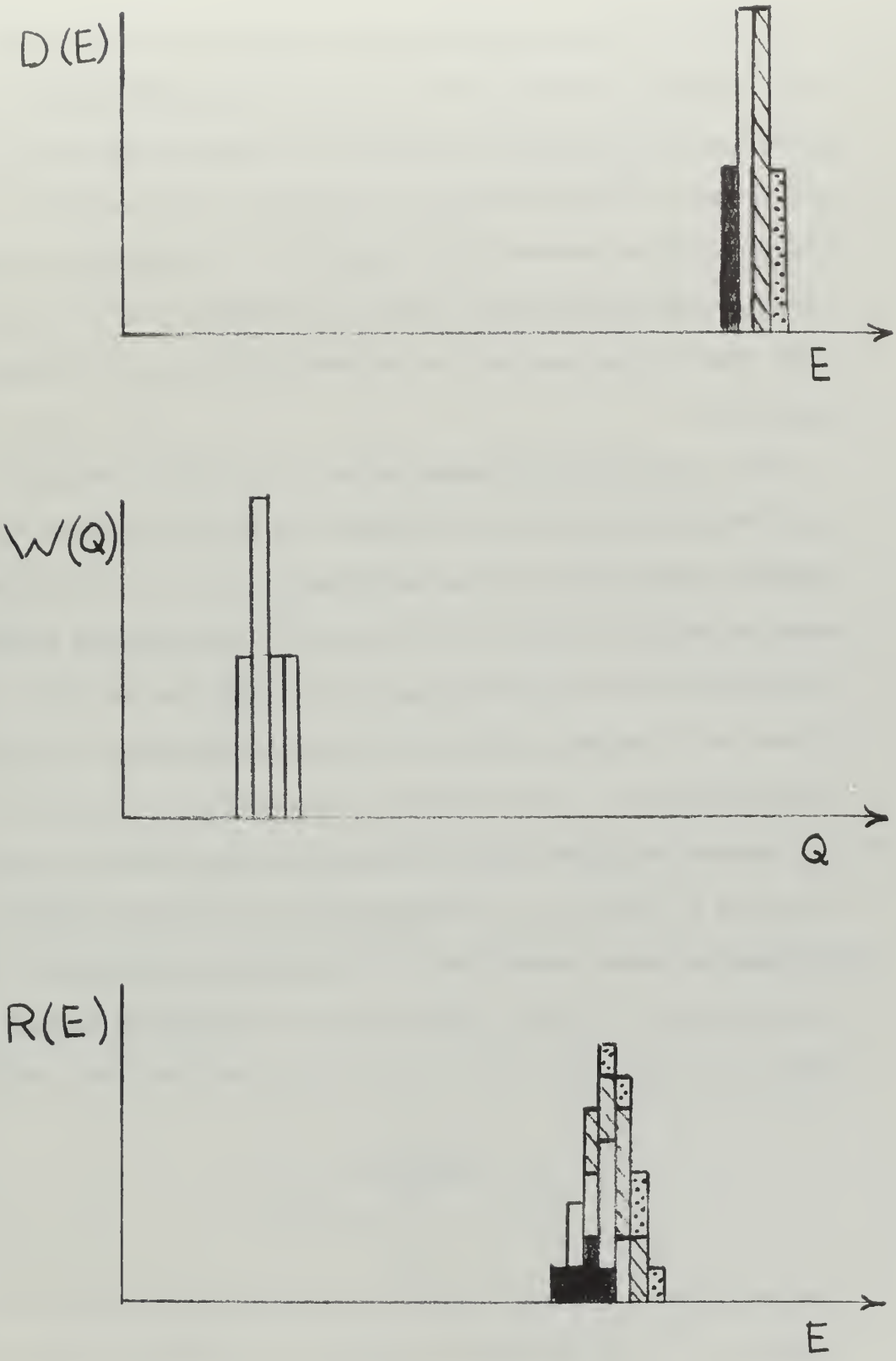


FIGURE 4. Histogram Process

The B & W curves used were those for $b^2 = 0$. Miller shows (c.f. his figure 8) that there is no significant difference between the curve predicted by the $b^2 = 0$ curves in B & W and $b^2 = 3$. In this work, $b^2$ ranged from a low of 0.088, corresponding to the thickest aluminum absorber (2.86 gms/cm$^2$) and 53.6 MeV; to a high of 0.934, corresponding to the thinnest copper absorber (0.71 gms/cm$^2$) at 94.3 MeV. From this one can see that the $b^2 = 0$ curves were appropriate.

The B & W curves are truncated at $\lambda = 15$. This results in minor discrepancies at the low energy tail of the predicted distribution. Therefore they were extended exponentially to $\lambda = 30$; by matching the amplitude and slope at $\lambda = 15$. This would not affect the predicted half-width but should more accurately represent the low energy tail. In one case it became necessary to extrapolate from $\alpha R = .25$ to obtain the curve for $\alpha R = .30$; for the Cu target with $t = 2.85$ gm-cm$^{-2}$.

Incident energies used in calculating other parameters were calculated by taking the value measured by the nuclear magnetic resonance probe and subtracting from it energy losses due to recoil; and ionization, excitation, and radiation when passing through the thin scattering foil. Recoil losses were calculated from the formula:

$$T = \frac{E_o^2}{M_c^2} \left( \frac{2 \sin^2 \theta/2}{1 + \frac{2E_o}{M_c^2} \sin^2 \theta/2} \right)$$

from Hofstadter (16), and checked by the relationship derived in Appendix A. In the Hofstadter formula $E_o$ is incident electron energy, M the mass of the aluminum nucleus, and $\theta$ was $90^o$ in this case. (This is not inconsistent with the opening remarks that in passage through

the absorber, the losses to recoil are insignificant. Very few of the electrons incident on a slab are scattered out to an angle of $90^{o}$, yet virtually all of the electrons incident on the absorbers have been scattered to an angle near $90^{o}$ by the foil. Because of the great difference in the masses the losses are small, typically 0.3 MeV loss at 94.5 MeV, but can't be neglected.) The values for ionization, excitation, and radiation losses were taken from Berger and Seltzer (17).

The B & W theoretical values reported in the Results section are not the $Q_o$ from the B & W theory because the B & W curves do not peak at $\lambda = 0$ and the predicted most probable energy loss is slightly greater than $Q_o$. The reported values were obtained by subtracting the energy value of the peak of the predicted curve from that of the peak of the incident beam. The predicted half widths were measured from the predicted curves. These predicted curves and the corresponding experimental points are shown as figures 5 through 28 in the Results section.

Distribution parameters for aluminum and copper are shown below as Tables III and IV.

TABLE III DISTRIBUTION PARAMETERS-ALUMINUM

| $t(gm/cm^2)$ | $E_i$(MeV) | $b^2$ | aR(MeV) | R(cm) |
|---|---|---|---|---|
| 0.730 | 96.93 | 0.374 | 0.0542 | 0.2743 |
| | 74.63 | 0.361 | 0.0542 | |
| | 53.57 | 0.345 | 0.0542 | |
| 1.441 | 96.93 | 0.190 | 0.1070 | 0.5418 |
| | 74.63 | 0.183 | 0.1070 | |
| | 53.57 | 0.175 | 0.1070 | |
| 2.146 | 96.93 | 0.127 | 0.1593 | 0.8067 |
| | 74.63 | 0.123 | 0.1593 | |
| | 53.57 | 0.117 | 0.1593 | |
| 2.859 | 96.93 | 0.096 | 0.2123 | 1.0749 |
| | 74.63 | 0.092 | 0.2123 | |
| | 53.57 | 0.088 | 0.2123 | |

Material: EC grade aluminum, purity 99.4%+

TABLE IV DISTRIBUTION PARAMETERS-COPPER

| $t(gm/cm^2)$ | $E_i$(MeV) | $b^2$ | aR(MeV) | R(cm) |
|---|---|---|---|---|
| 0.711 | 94.30 | 0.934 | 0.050 | 0.080 |
| | 74.76 | 0.904 | 0.050 | |
| | 52.84 | 0.858 | 0.050 | |
| 1.423 | 94.30 | 0.467 | 0.09999 | 0.160 |
| | 74.76 | 0.452 | 0.09999 | |
| | 52.84 | 0.429 | 0.100 | |
| 2.134 | 94.30 | 0.311 | 0.14999 | 0.240 |
| | 74.76 | 0.301 | 0.14999 | |
| | 52.84 | 0.286 | 0.150 | |
| 2.845 | 94.30 | 0.233 | 0.19998 | 0.320 |
| | 74.76 | 0.226 | 0.19999 | |
| | 52.84 | 0.214 | 0.19999 | |

Material: Hard drawn copper, purity 99.0%+

The values presented as measured or observed number of counts are the number obtained by taking the raw data, correcting it for the effect of losses due to high counting rate, and subtracting off the background. For aluminum, a method similar to that used by Miller was used to correct for high counting rate. His relationship was:

$$N = EN\left(1 + \left(\frac{EN}{T}\right)\frac{3.3}{1160}\right)$$

where N is the corrected number, EN is the raw data, and T is the time taken to count EN counts. The term $\frac{EN}{T}$ is the counting rate at which the

number EN was counted. The factor $\frac{3.3}{1160}$ was derived by varying the counting rate with a standard set up and observing the response of the counters. This response was graphed (counts versus counting rate) and the slope of this graph determined the numerical value of the correction factor.

The relationship used for aluminum in this case was:

$$N = EN \div (1 - (\frac{F}{1000} \times \frac{EN}{T})) - \text{Background}$$

Here $\frac{F}{1000}$ is the numerical value obtained by graphing the response of the counters after all data was taken at each energy.

For copper the beam was kept down to a value which would produce a maximum of 6 counts per second. When this is done, the correction becomes:

$$r_t = r_o(1 + .6r_o)$$

where $r_t$ is the true number of counts per machine pulse, and $r_o$ is the number of counts per machine pulse observed. This requires converting the observed counts and time to counts per machine pulse, but as shown by Browman (18) it will yield more accurate results because it is not dependent on the instantaneous shape of the machine pulses. Computer programs for correcting the observed counts are included as Appendices B and C.

## V. RESULTS

The values predicted by theory and experimental results of most probable energy loss and distribution half widths for both aluminum and copper are shown in tables V and VI. The column headed S under $Q_p$ is the Sternheimer prediction, B & W is the Blunck & Westphal prediction.

As one can readily see, the measured data fit the B & W theory well, and differ significantly from the Sternheimer predictions. When considering energy loss in aluminum, the observed data differ from the B & W curves by an average of 2 1/4% and differ from Sternheimer by 7%. With copper, the difference is more dramatic; average difference from B & W is 1 1/2%, average difference from Sternheimer is 8 1/3%. The half-widths observed agree with the B & W theory also. Of the 24 half-widths measured, 6 fall further away from the predicted value than the error limits assigned to the observed points. Because of the way the half width predictions were determined, error limits should be assigned to the predicted values. These come from the uncertainty in the exact energy of the incident beam. If a $\pm$ 0.3% value is used as the uncertainty in energy (see Oberdier (19) and Miller (1)), then this would result in only three of these points being out of the error limits. This is quite good agreement. If there is a systematic error it is that the observed half widths are narrower than those predicted and is the opposite effect from that observed by Breuer.

In order to determine the tolerances in the observed energy losses and half widths, error bars were put on the observed points, and extreme case curves were plotted.

TABLE V ENERGY LOSS IN ALUMINUM

| | | $Q_p$ (MeV) | | | HW (MeV) | |
|---|---|---|---|---|---|---|
| $E_i$ (MeV) | t ($gm/cm^2$) | B & W | S | Experiment | Theory | Experiment |
| 96.93 | 0.730 | 1.082 | 0.977 | 1.17 | 0.67 | 0.66 |
| | 1.441 | 2.166 | 2.002 | 2.16 | 1.00 | 1.01 |
| | 2.146 | 3.247 | 3.044 | 3.24 | 1.32 | 1.19 |
| | 2.859 | 4.370 | 4.117 | 4.32 | 1.79 | 1.48 |
| 74.63 | 0.730 | 1.066 | 0.976 | 1.04 | 0.59 | 0.51 |
| | 1.441 | 2.094 | 2.000 | 2.18 | 0.91 | 0.91 |
| | 2.146 | 3.174 | 3.041 | 3.17 | 1.21 | 1.08 |
| | 2.859 | 4.297 | 4.113 | 4.26 | 1.61 | 1.38 |
| 53.57 | 0.730 | 1.051 | 0.974 | 1.03 | 0.47 | 0.49 |
| | 1.441 | 2.088 | 1.996 | 2.16 | 0.75 | 0.75 |
| | 2.146 | 3.172 | 3.036 | 3.18 | 0.99 | 1.02 |
| | 2.859 | 4.347 | 4.106 | 4.21 | 1.35 | 1.32 |

TABLE VI ENERGY LOSS IN COPPER

| | | $Q_p$ (MeV) | | HW(MeV) | | |
|---|---|---|---|---|---|---|
| $E_i$ (MeV) | t ($gm/cm^2$) | B & W | S | Experiment | Theory | Experiment |
| 94.30 | 0.711 | 1.014 | 0.840 | 0.95 | 0.69 | 0.74 |
| | 1.423 | 1.947 | 1.750 | 1.94 | 1.12 | 0.99 |
| | 2.134 | 2.956 | 2.685 | 2.93 | 1.62 | 1.47 |
| | 2.845 | 4.082 | 3.637 | 4.00 | 2.31 | 1.75 |
| 74.76 | 0.711 | 0.913 | 0.839 | 0.92 | 0.62 | 0.66 |
| | 1.423 | 1.894 | 1.747 | 1.91 | 1.01 | 1.07 |
| | 2.134 | 2.903 | 2.681 | 2.92 | 1.51 | 1.43 |
| | 2.845 | 3.978 | 3.633 | 3.98 | 2.16 | 1.98 |
| 52.84 | 0.711 | 0.950 | 0.837 | 0.94 | 0.50 | 0.52 |
| | 1.423 | 1.880 | 1.743 | 1.87 | 0.82 | 0.84 |
| | 2.134 | 2.886 | 2.675 | 2.87 | 1.27 | 1.16 |
| | 2.845 | 3.959 | 3.624 | 3.80 | 1.91 | 1.75 |

Plots of the predicted curves and observed points are included as figures 5 through 28. These were plotted by the IBM 360 computer. A plot of predicted and observed half widths with the aluminum absorbers is figure 29; copper, figure 30.

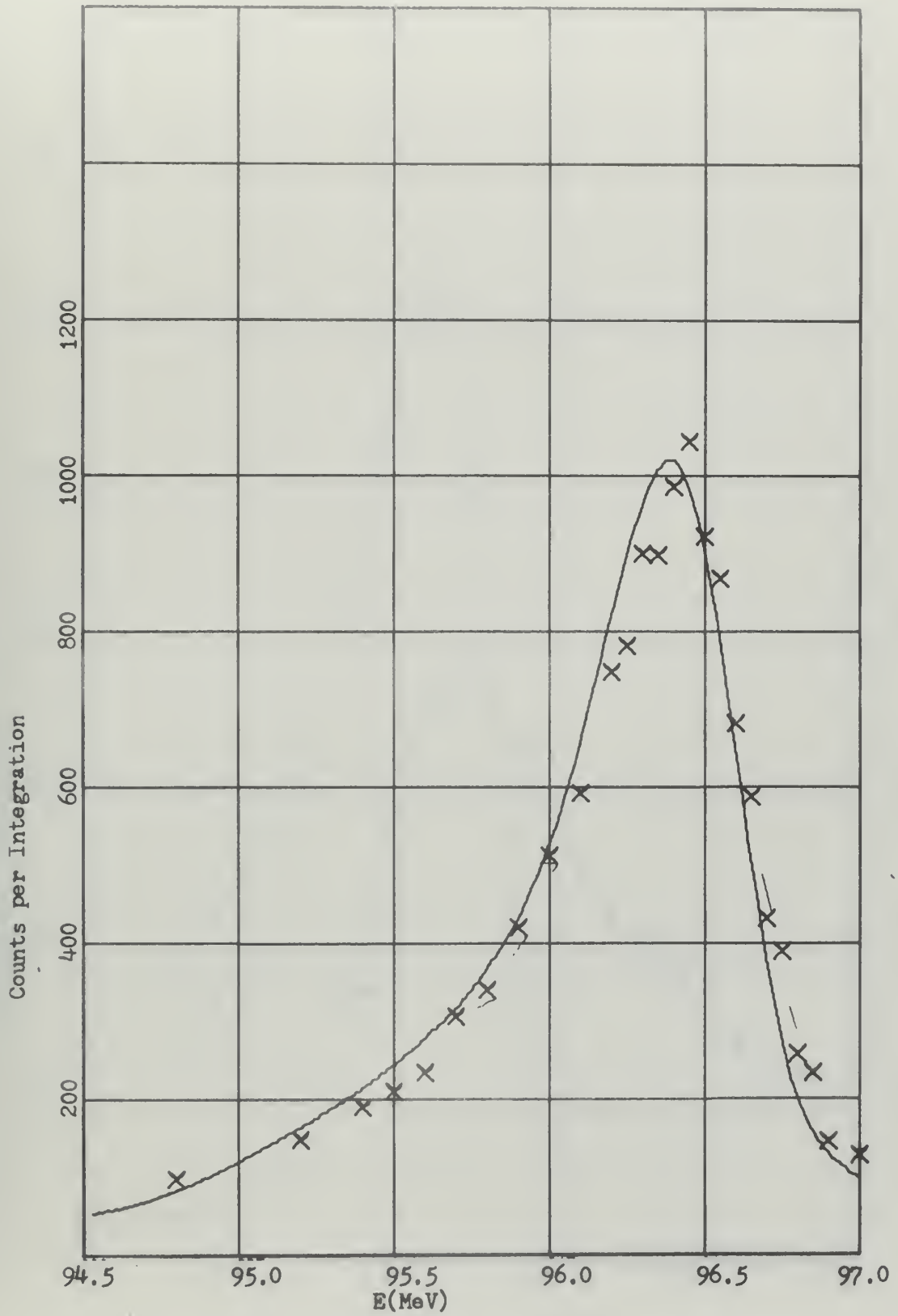


Figure 5. Predicted Distribution, Al
$t=0.730$ gm/cm$^2$ $E_i = 96.93$ MeV

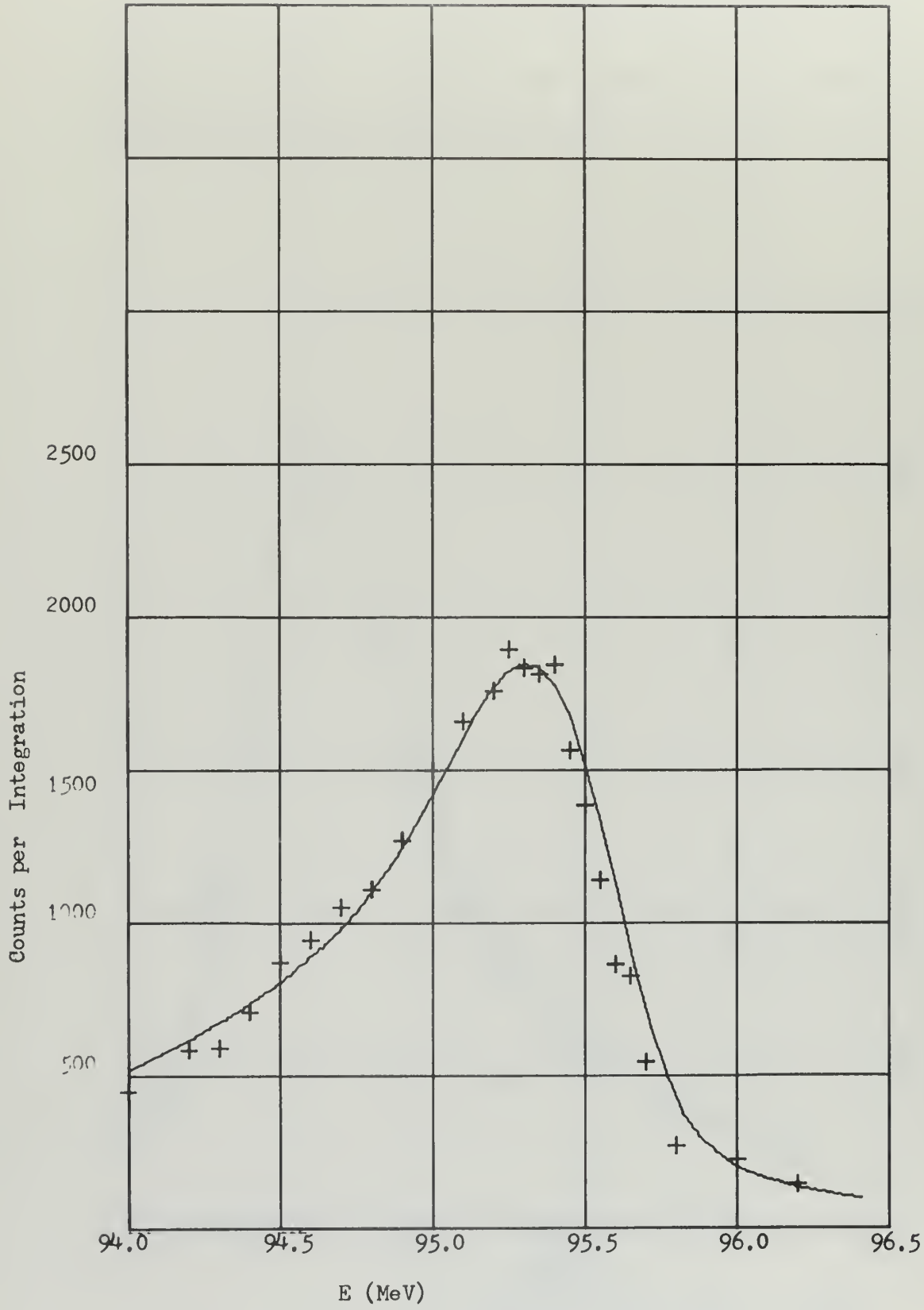


Figure 6. Predicted Distribution, Al
$t = 1.441$ gm/cm$^2$ $E_i = 96.93$ MeV

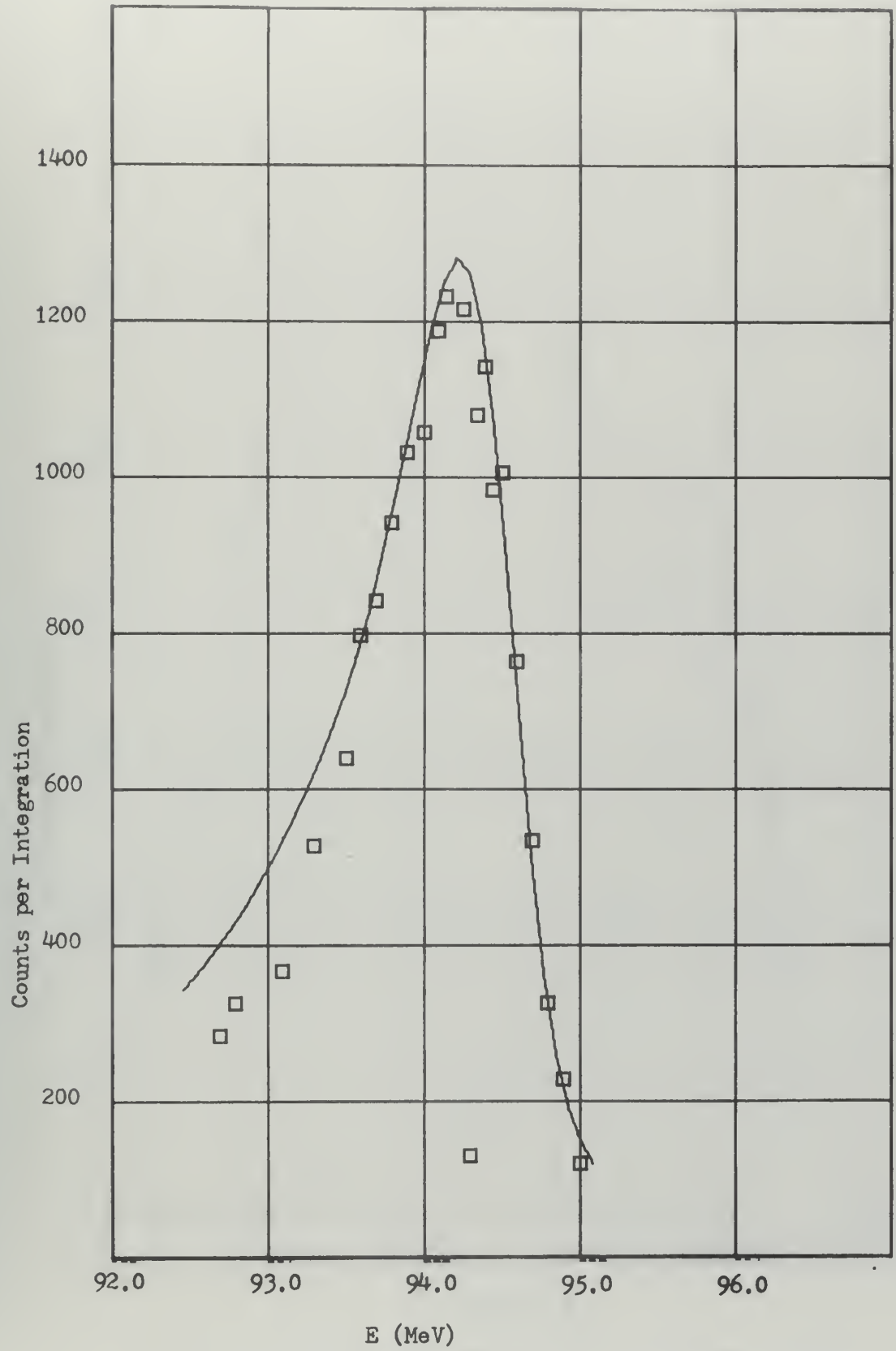


Figure 7. Predicted Distribution, Al
$t = 2.146\ gm/cm^2$ $E_i = 96.93$ MeV

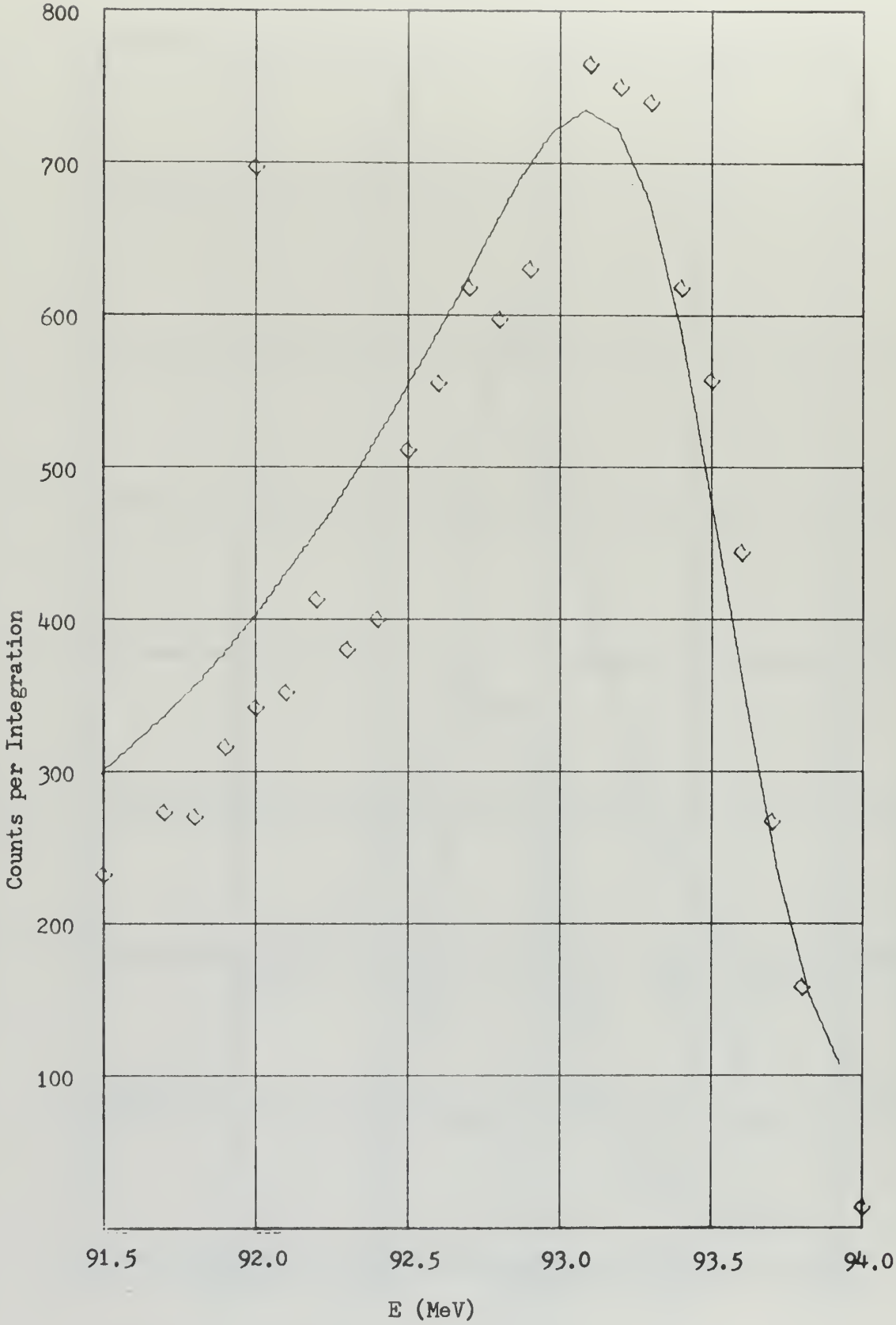


Figure 8. Predicted Distribution Al
$t = 2.859\ gm/cm^2$ $E_i = 96.93$ MeV

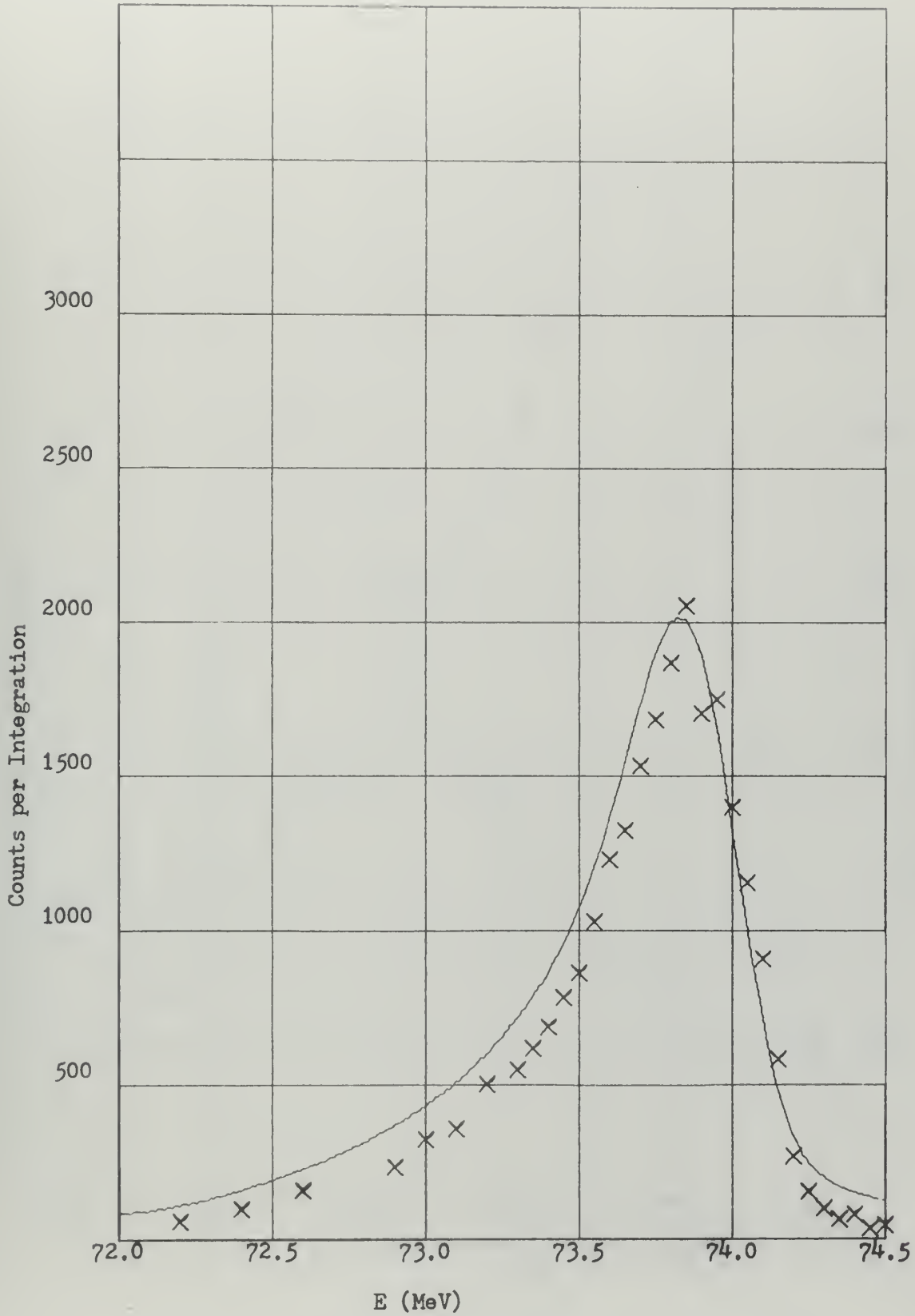


Figure 9. Predicted Distribution, Al
t=0.730 MeV gm/cm$^2$ $E_i$= 74.63 MeV

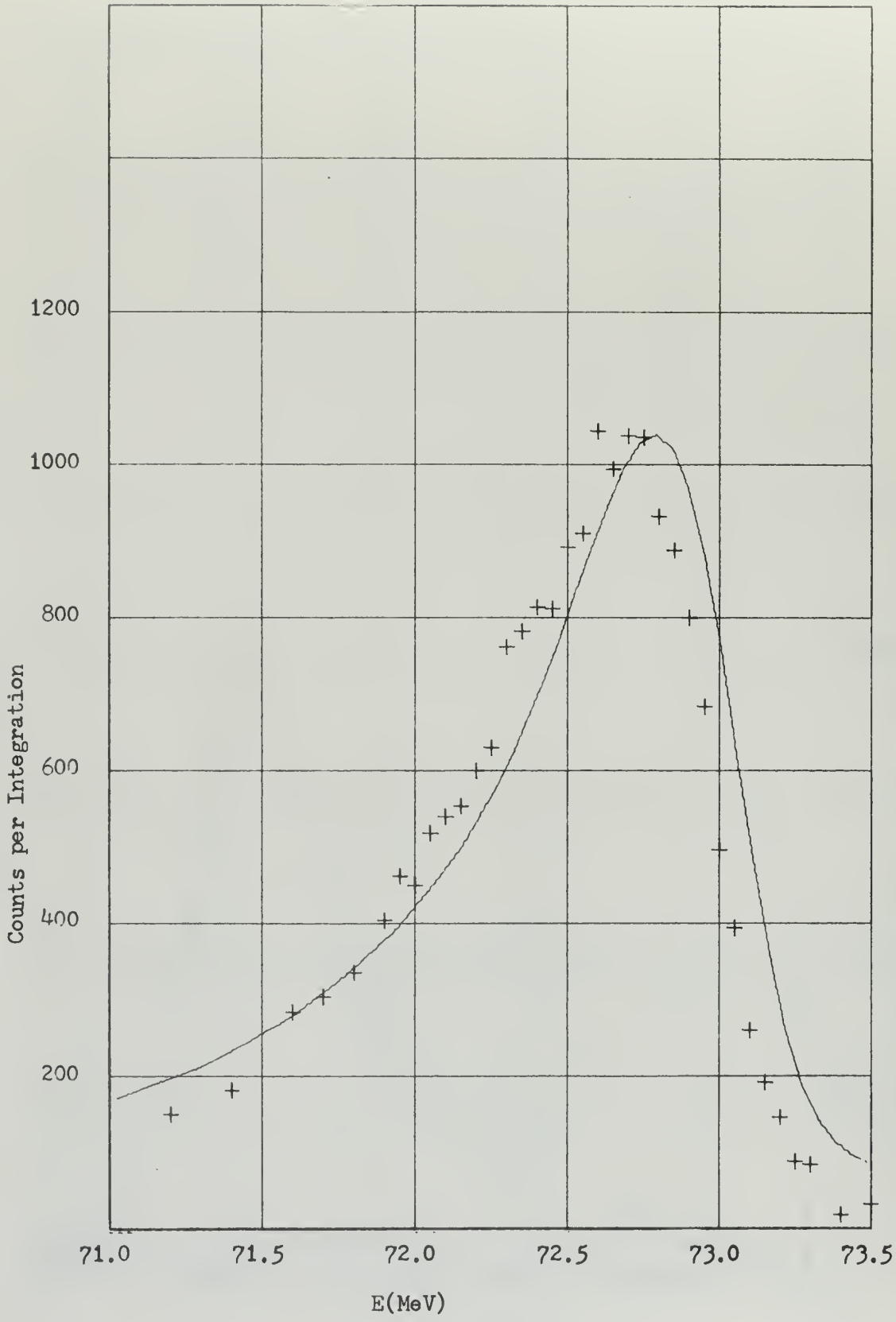


Figure 10. Predicted Distribution, Al
$t = 1.441$ gm/cm$^2$ $E_i = 74.63$ MeV

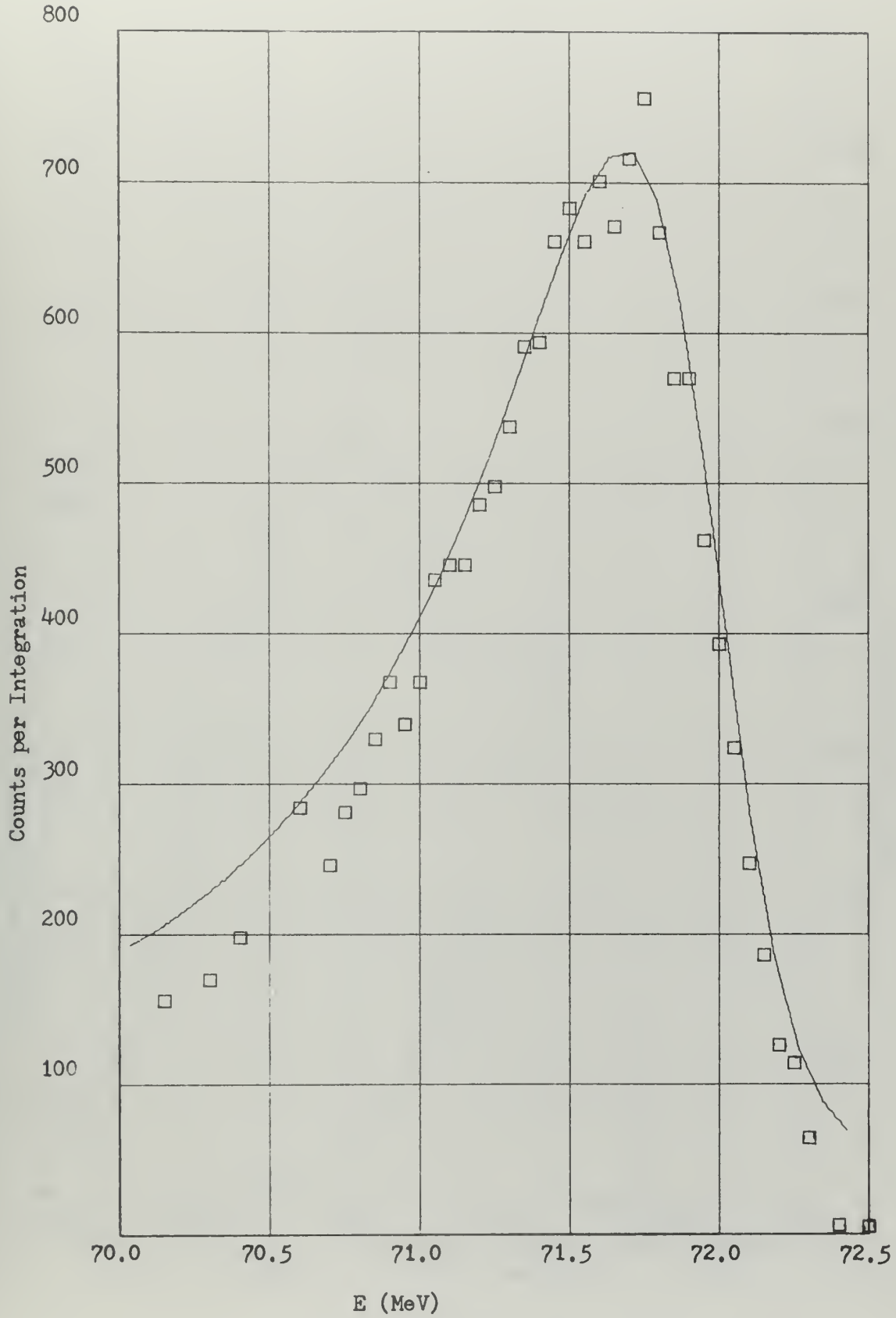


Figure 11. Predicted Distribution, Al
t= 2.146 gm/cm$^2$ $E_i$= 74.63 MeV

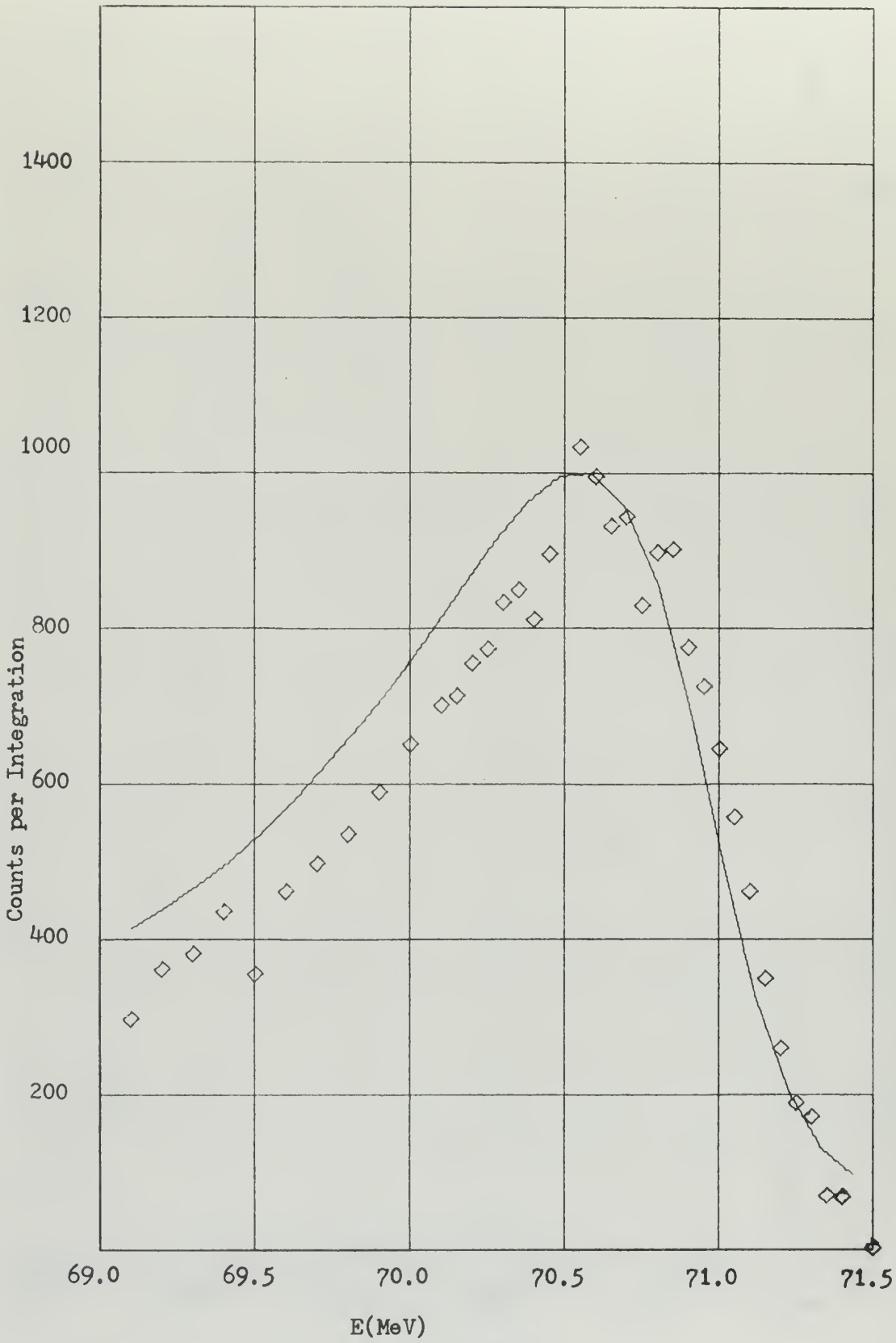


Figure 12. Predicted Distribution, Al
t= 2.859 gm/cm$^2$ $E_i$= 74.63 MeV

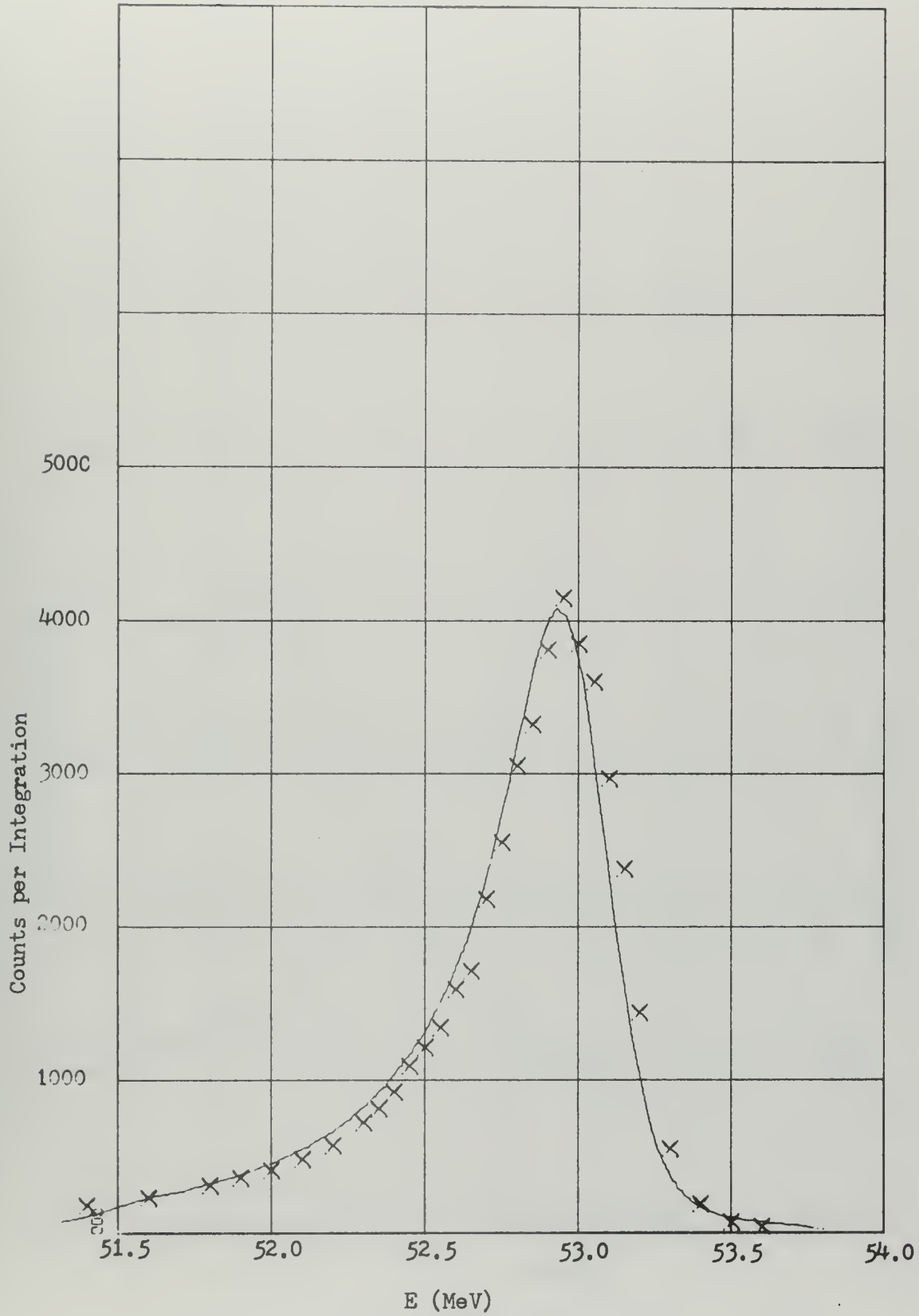


Figure 13. Predicted Distribution, Al
$t = 0.730$ gm/cm$^2$ $E_i = 53.57$ MeV

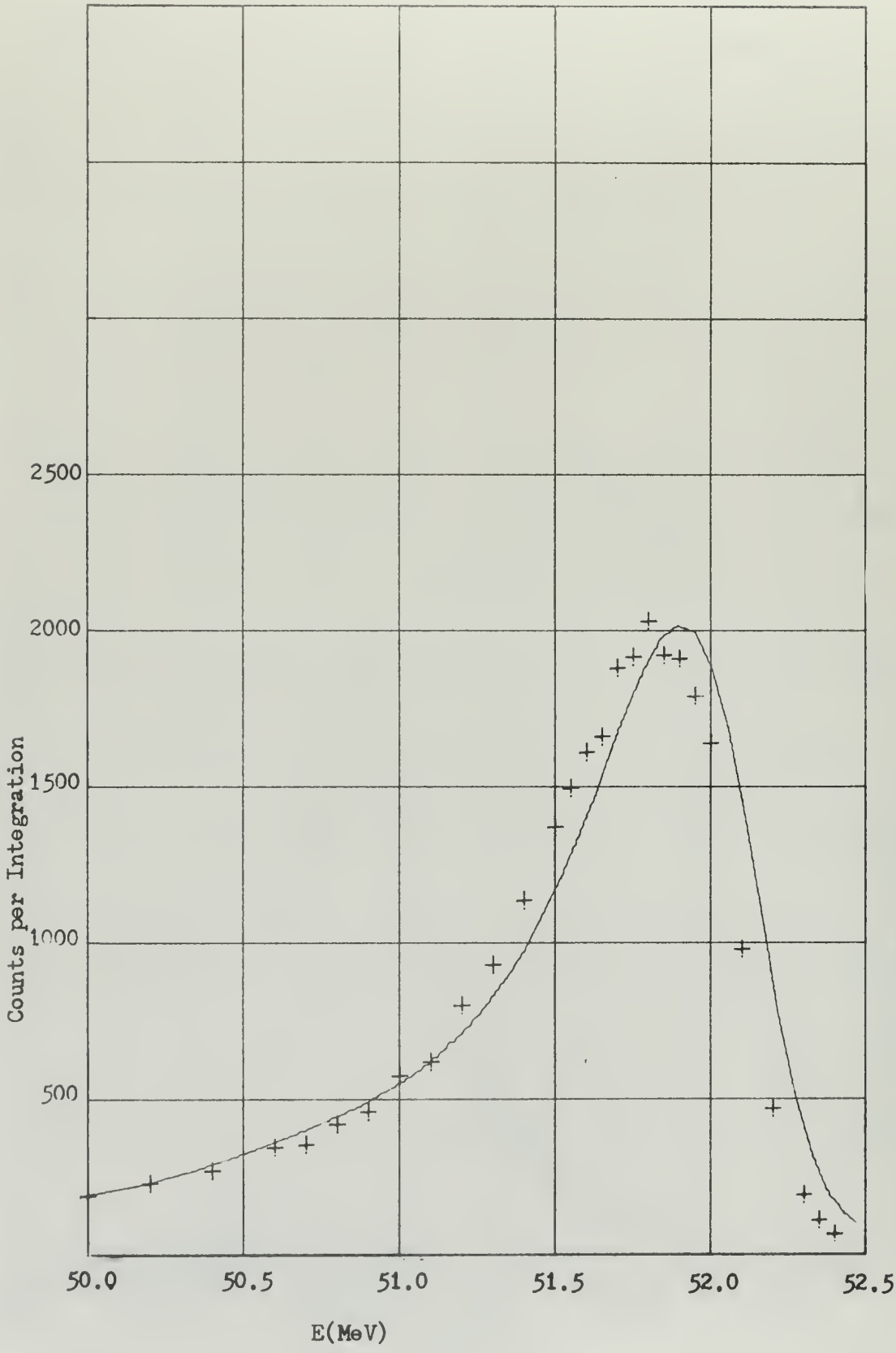


Figure 14. Predicted Distribution, Al
t= 1.441 gm/cm$^2$ $E_i$= 53.57 MeV

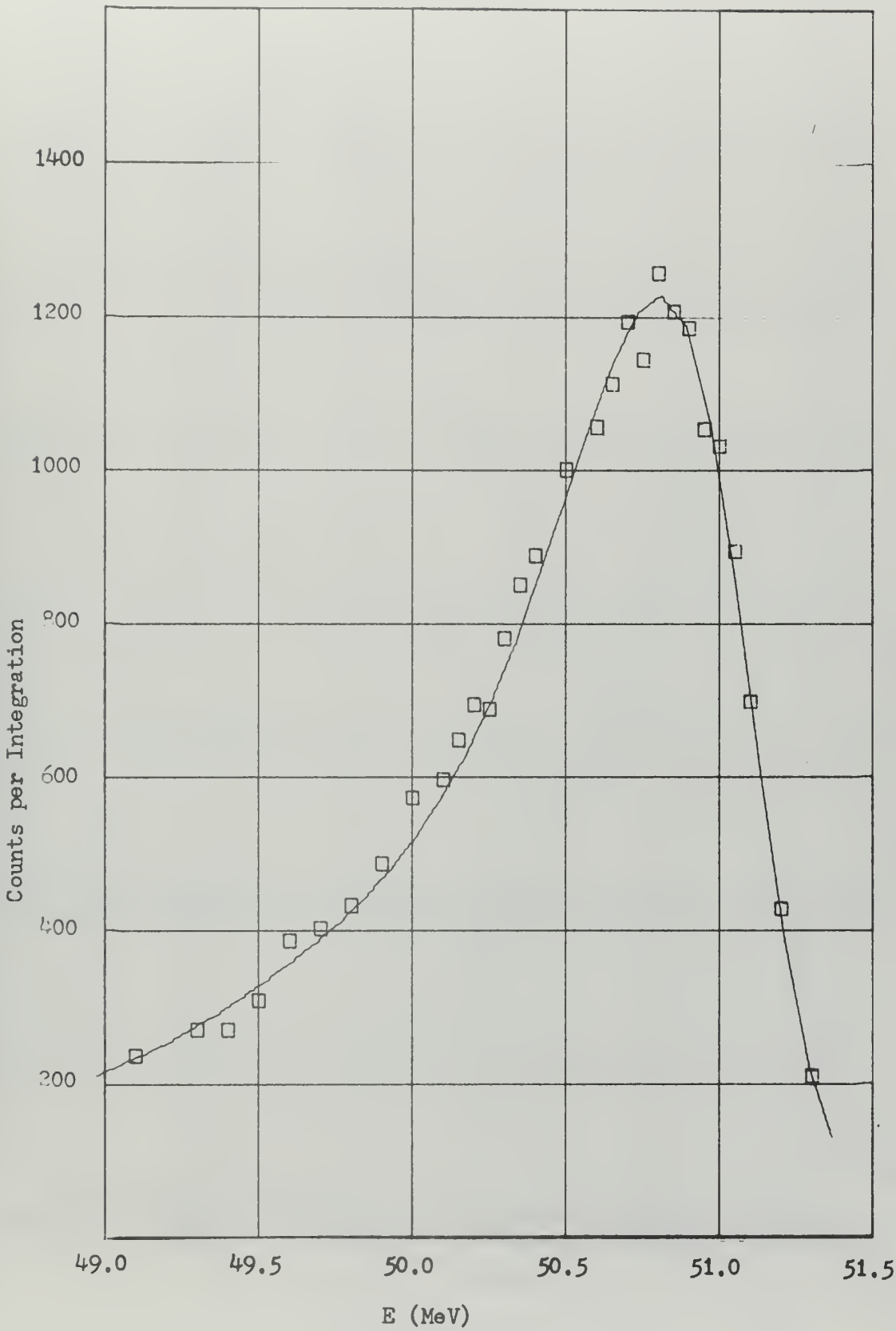


Figure 15. Predicted Distribution, Al
$t = 2.146\ gm/cm^2$ $E_i = 53.57$ MeV

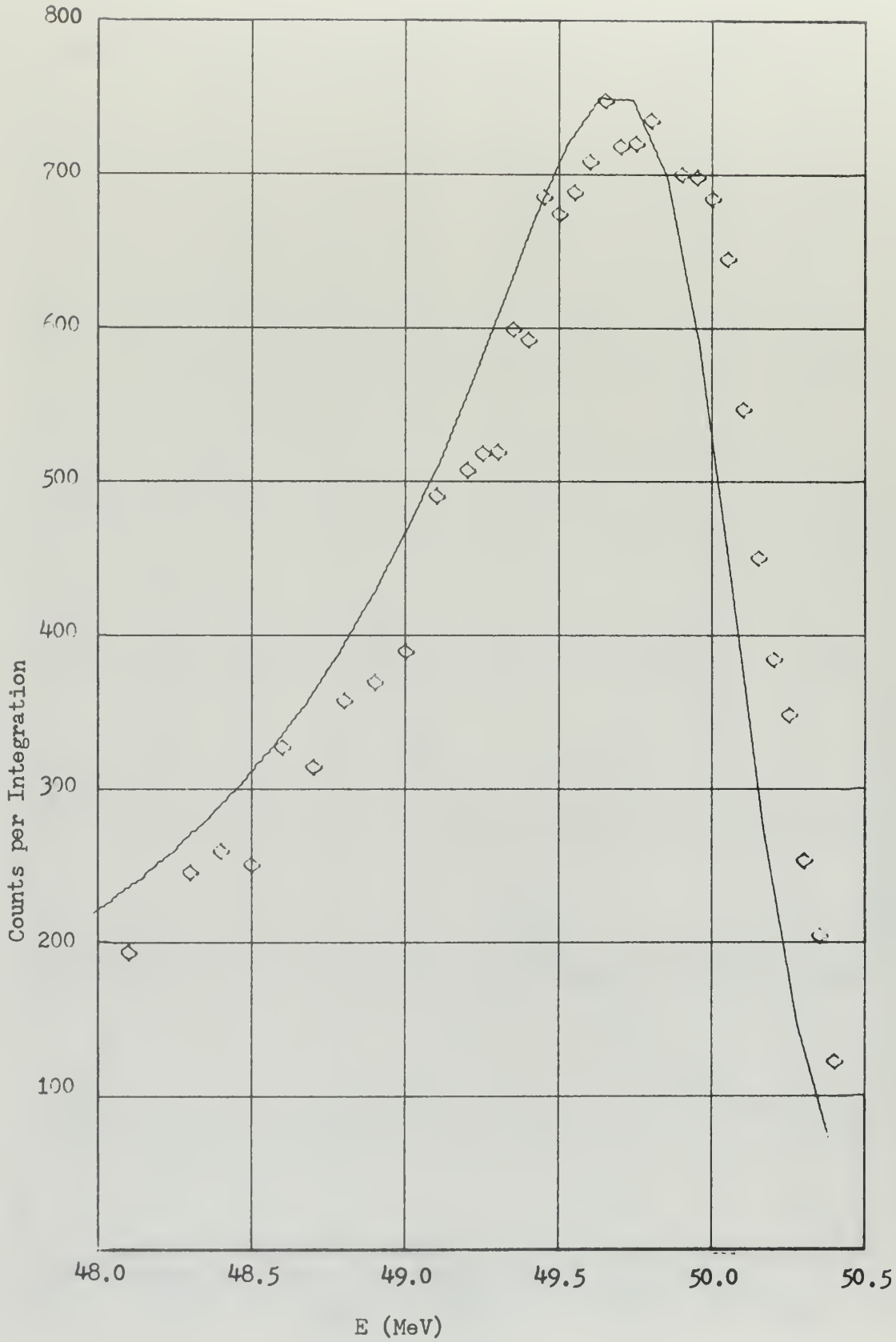


Figure 16. Predicted Distribution, Al
t= 2.859 gm/cm$^2$ $E_i$= 53.57 MeV

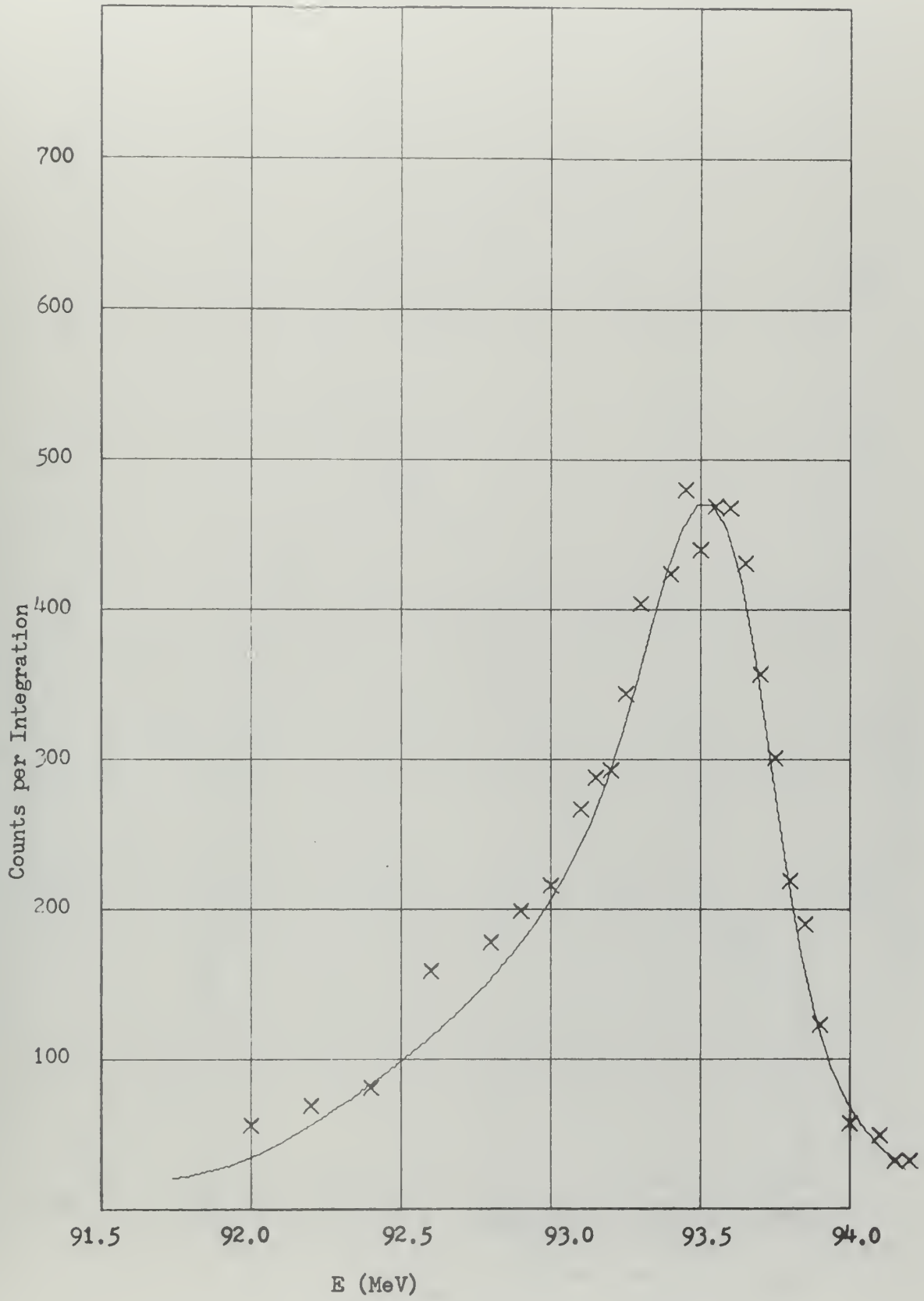


Figure 17. Predicted Distribution, Cu
t= 0.711 gm/cm$^2$ $E_i$= 94.30 MeV

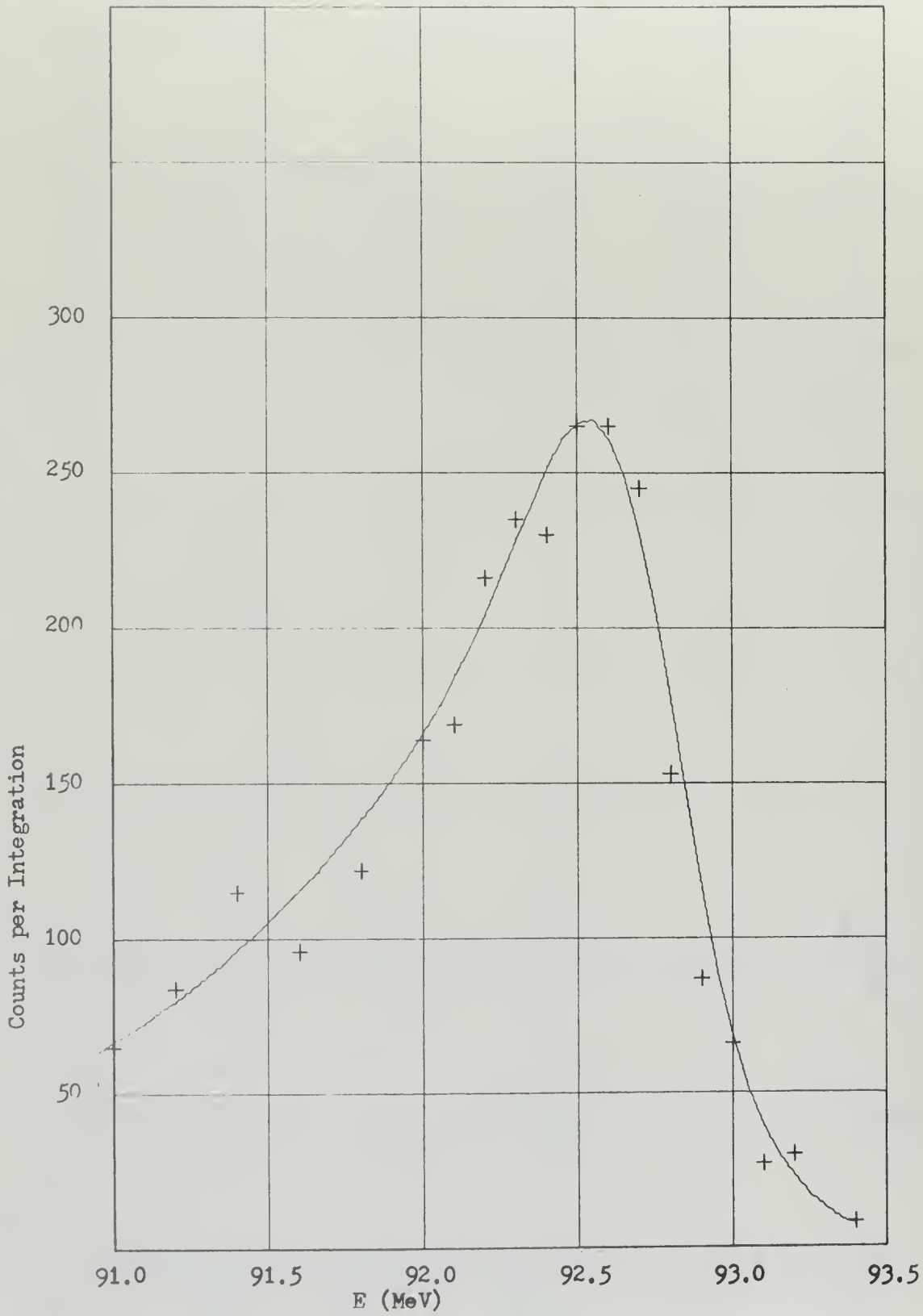


Figure 18. Predicted Distribution, Cu
$t = 1.423\ gm/cm^2$ $E_i = 94.30$ MeV

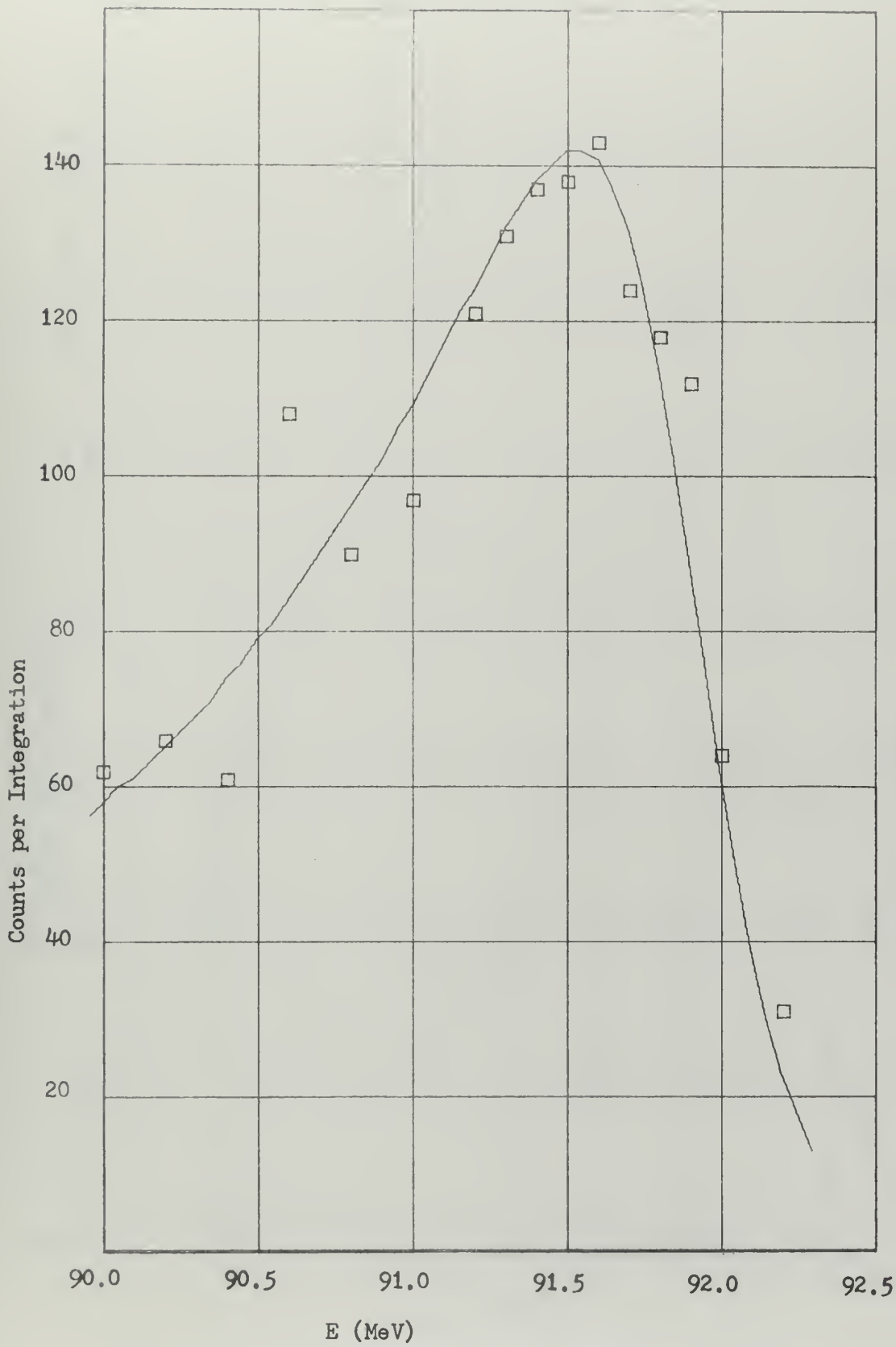


Figure 19. Predicted Distribution, Cu
$t = 2.134$ gm/cm$^2$ $E_i = 94.30$ MeV

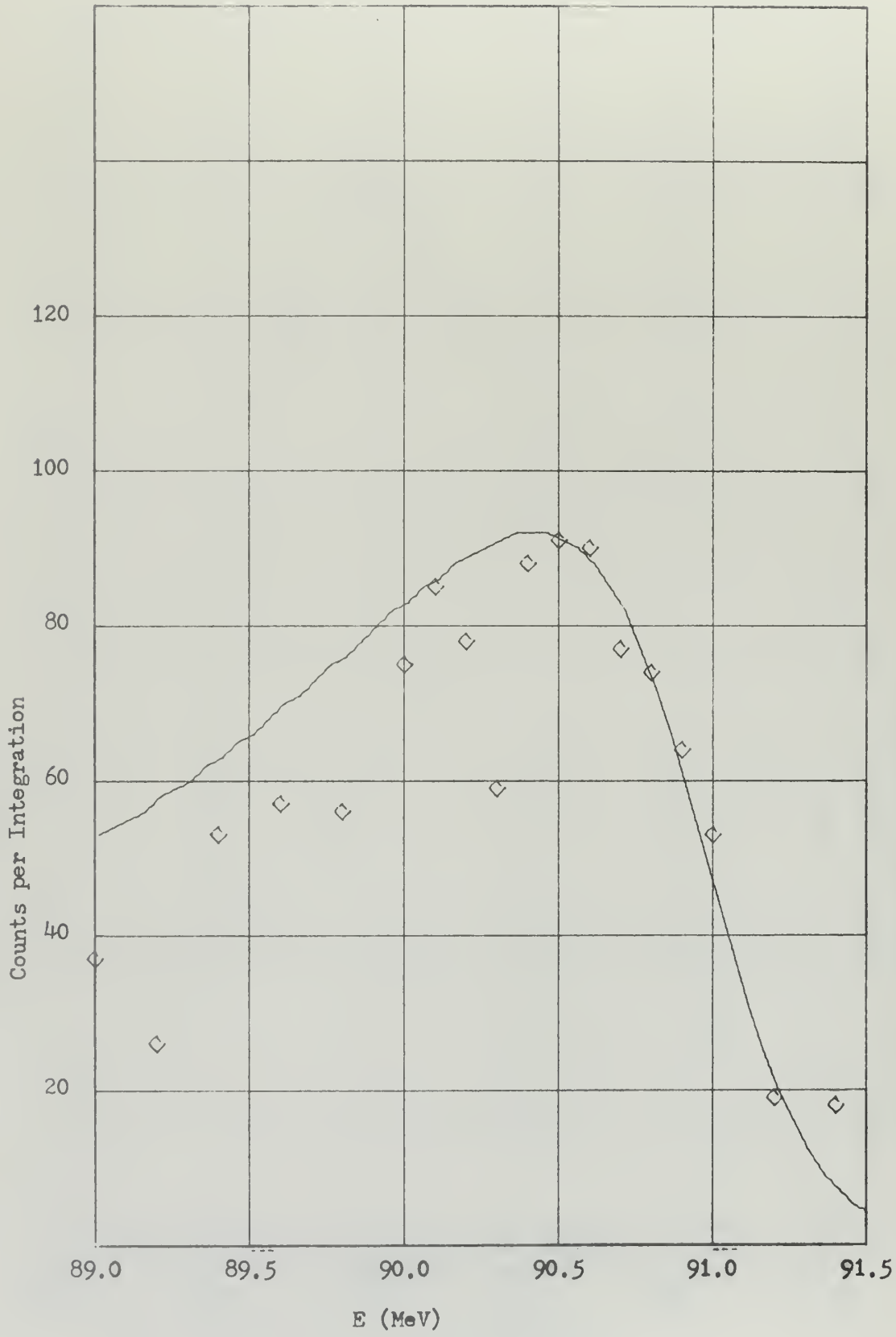


Figure 20. Predicted Distribution, Cu
$t = 2.845$ gm/cm$^2$ $E_i = 94.30$ MeV

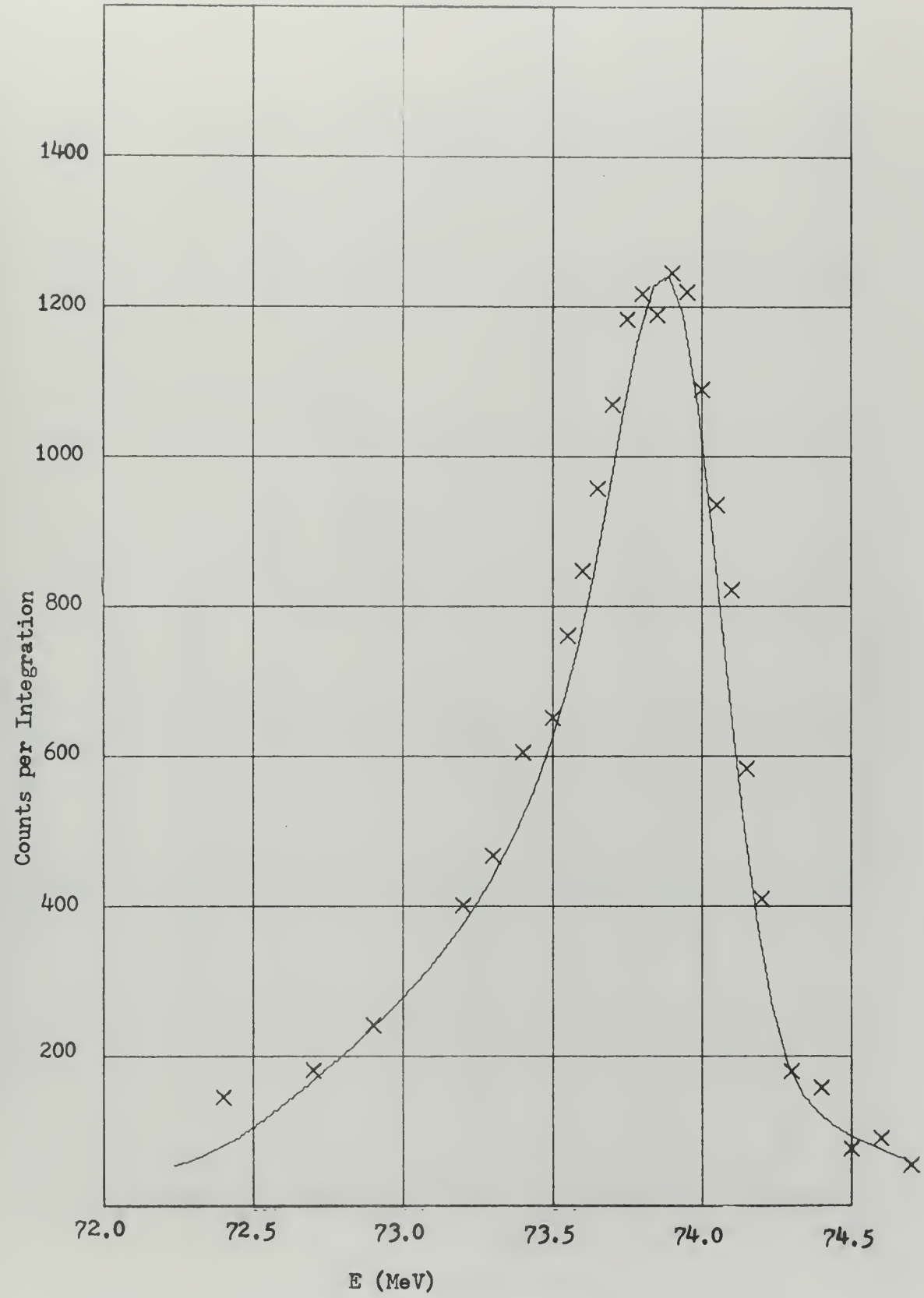


Figure 21. Predicted Distribution, Cu
t= 0.711 gm/cm2 $E_i$= 74.76 MeV

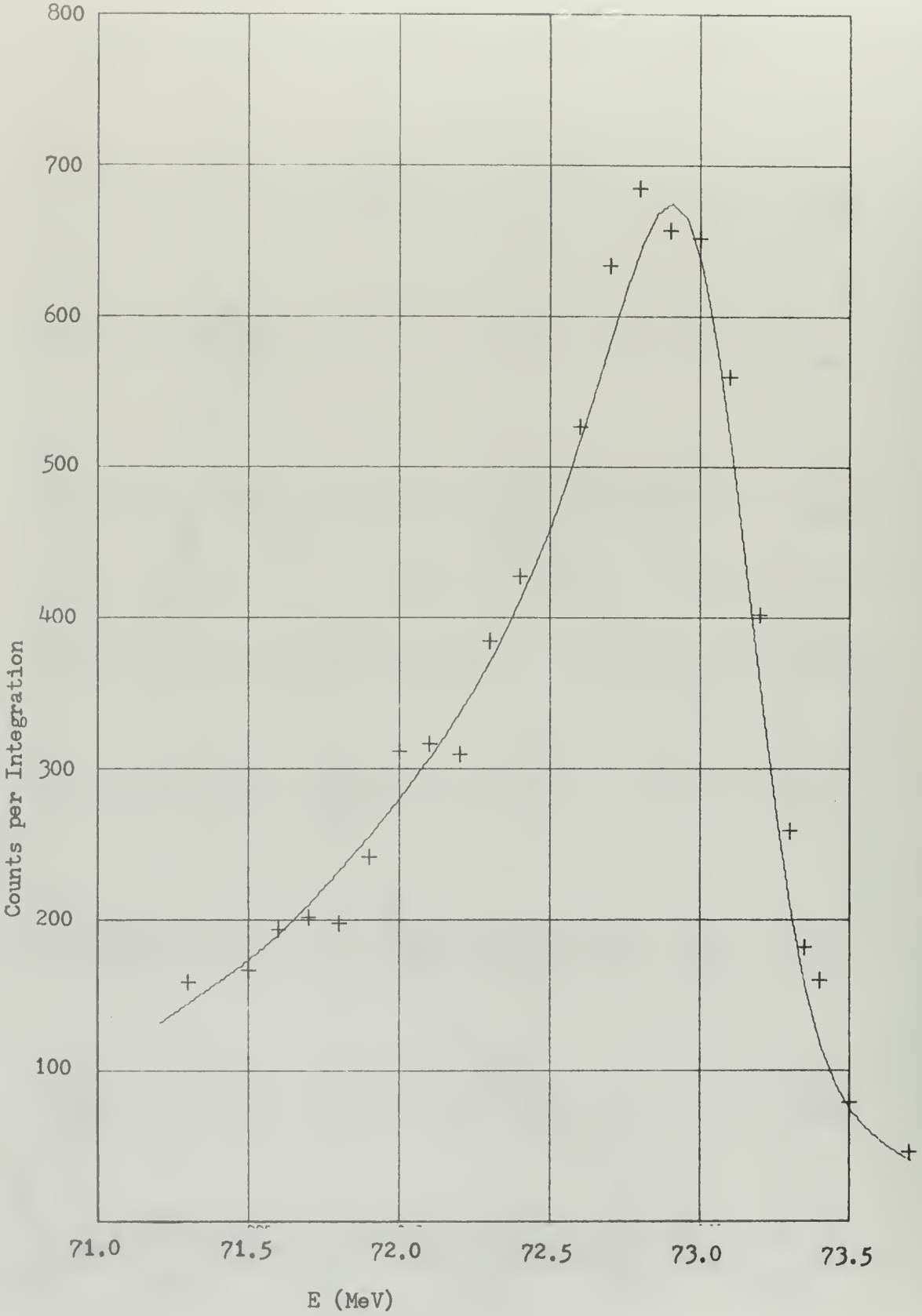


Figure 22. Predicted Distribution Cu
$t = 1.423$ gm/cm$^2$ $E_i = 74.76$ MeV

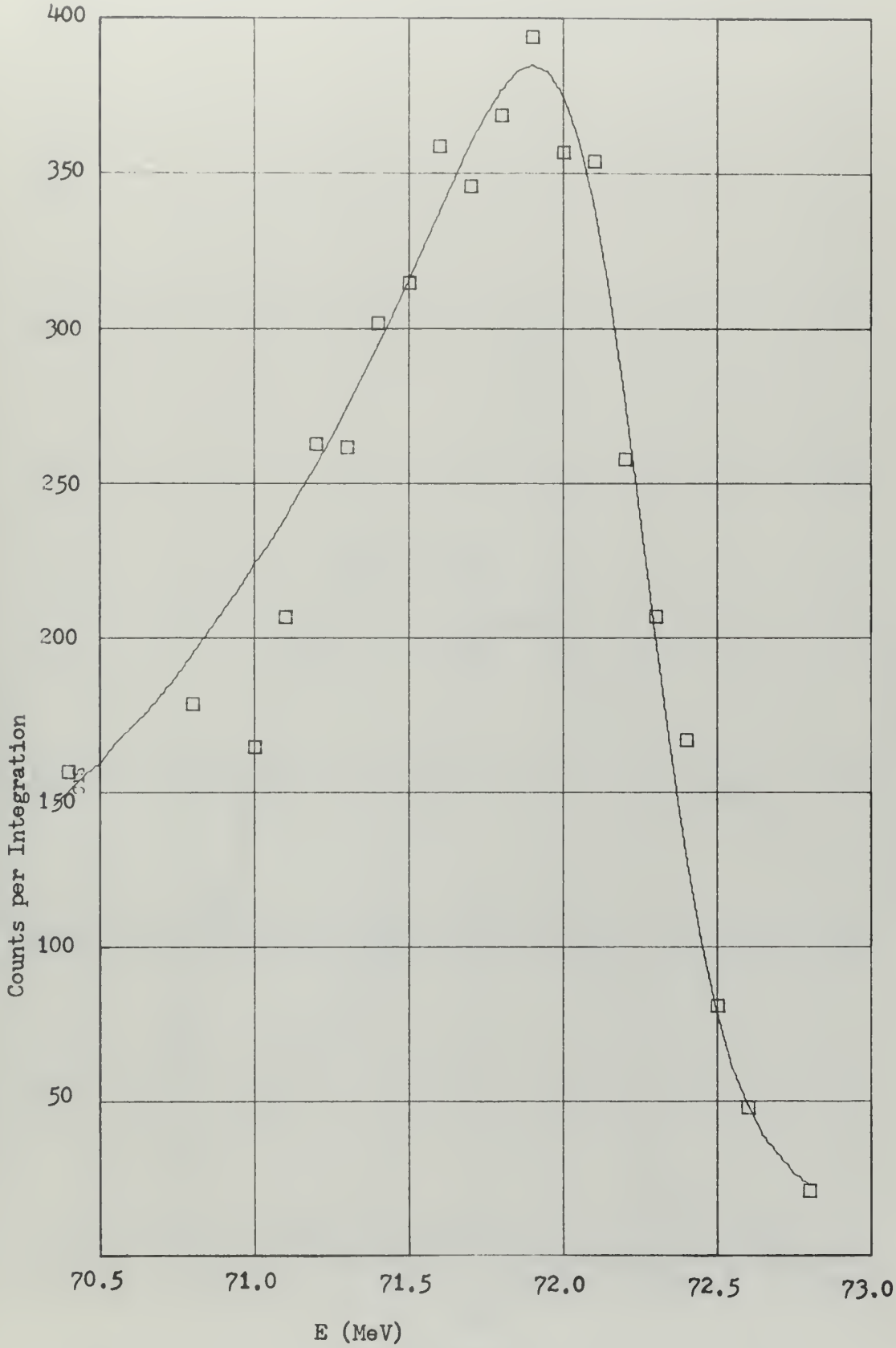


Figure 23. Predicted Distribution, Cu
t= 2.134 gm/cm$^2$ $E_i$= 74.76 MeV

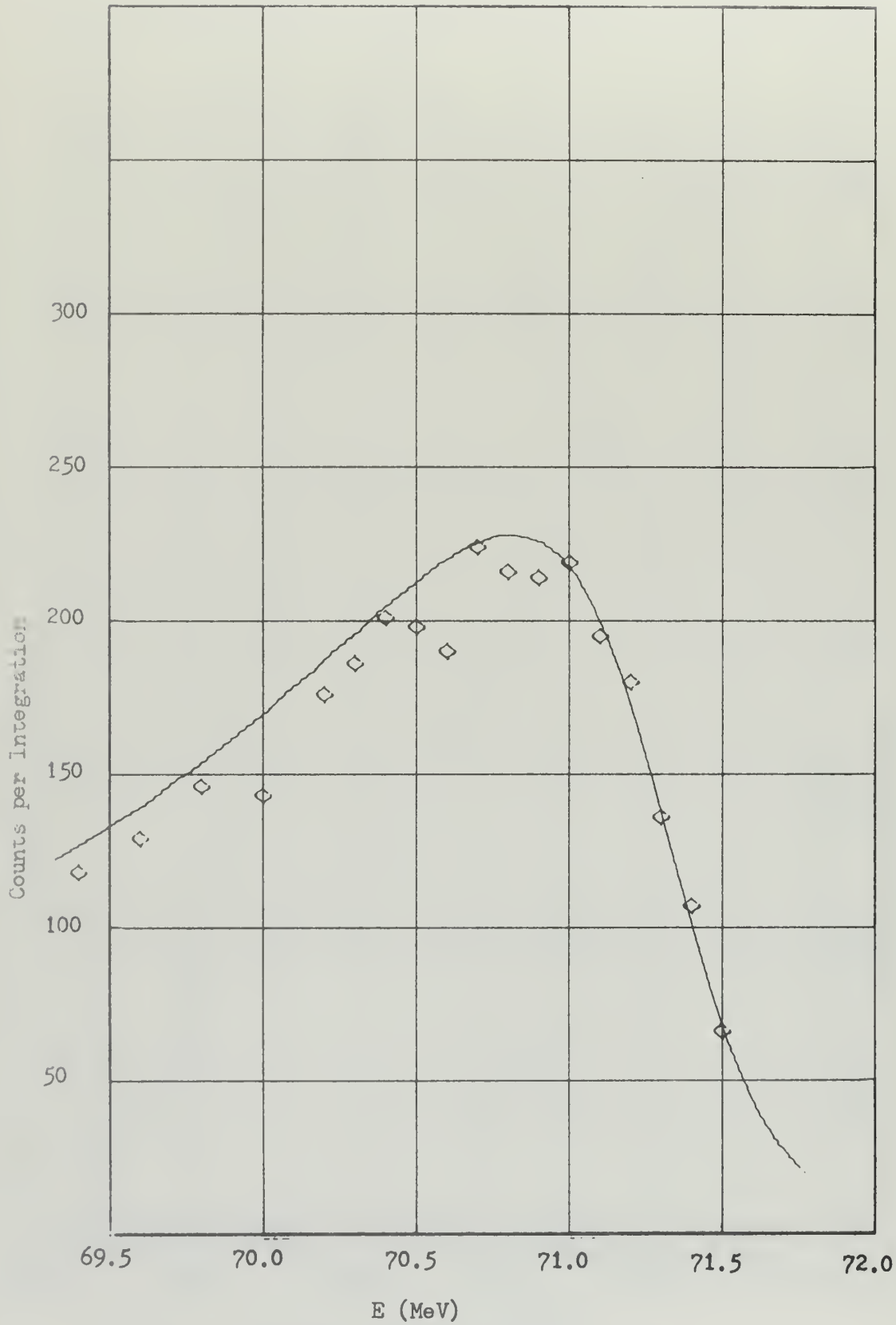


Figure 24. Predicted Distribution, Cu
t= 2.845 gm/cm$^2$ $E_i$= 74.76 MeV

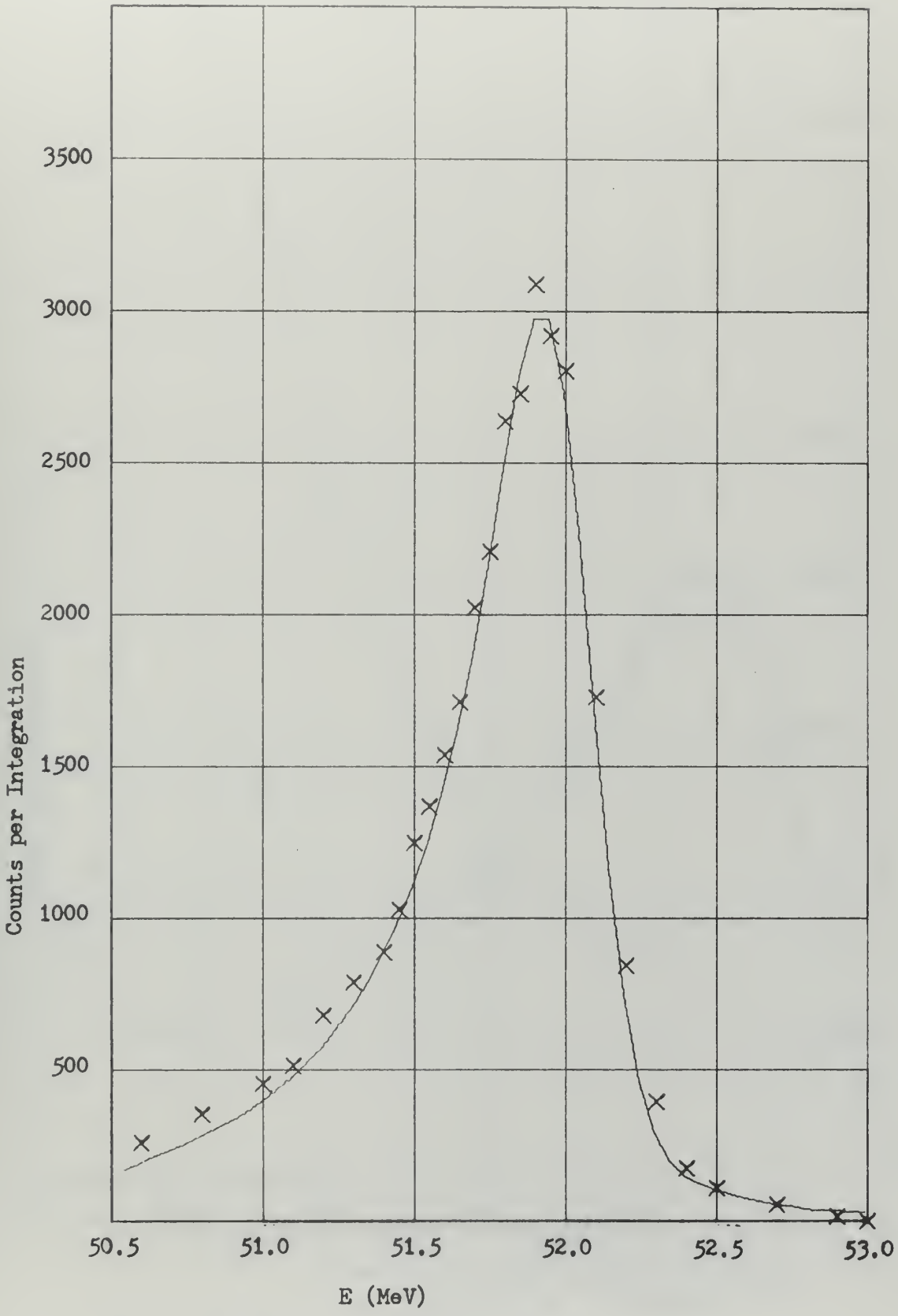


Figure 25. Predicted Distribution, Cu
t= 0.711 gm/cm$^2$ $E_i$= 52.84 MeV

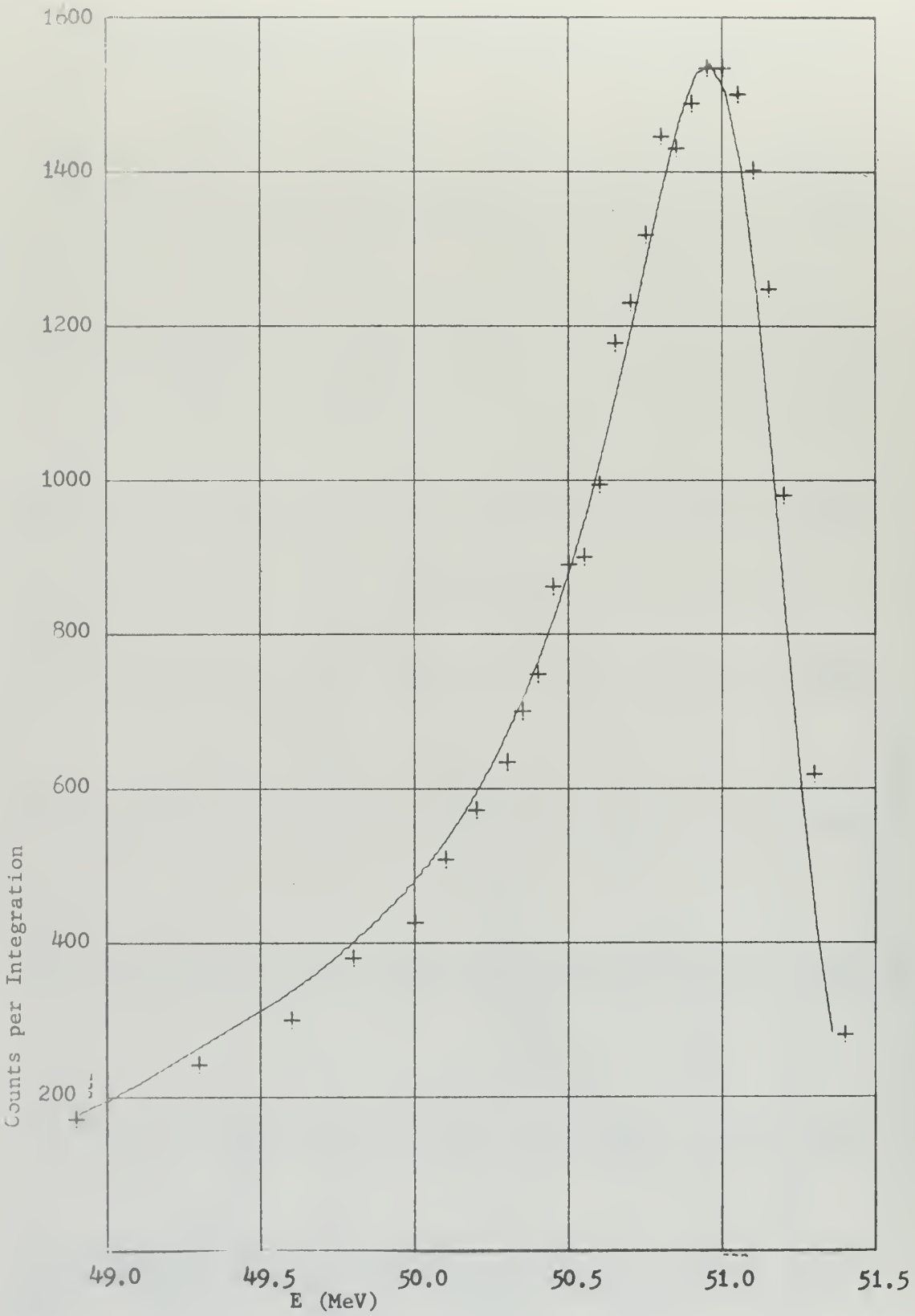


Figure 26. Predicted Distribution, Cu
t= 1.423 gm/cm$^2$ $E_i$= 52.84 MeV

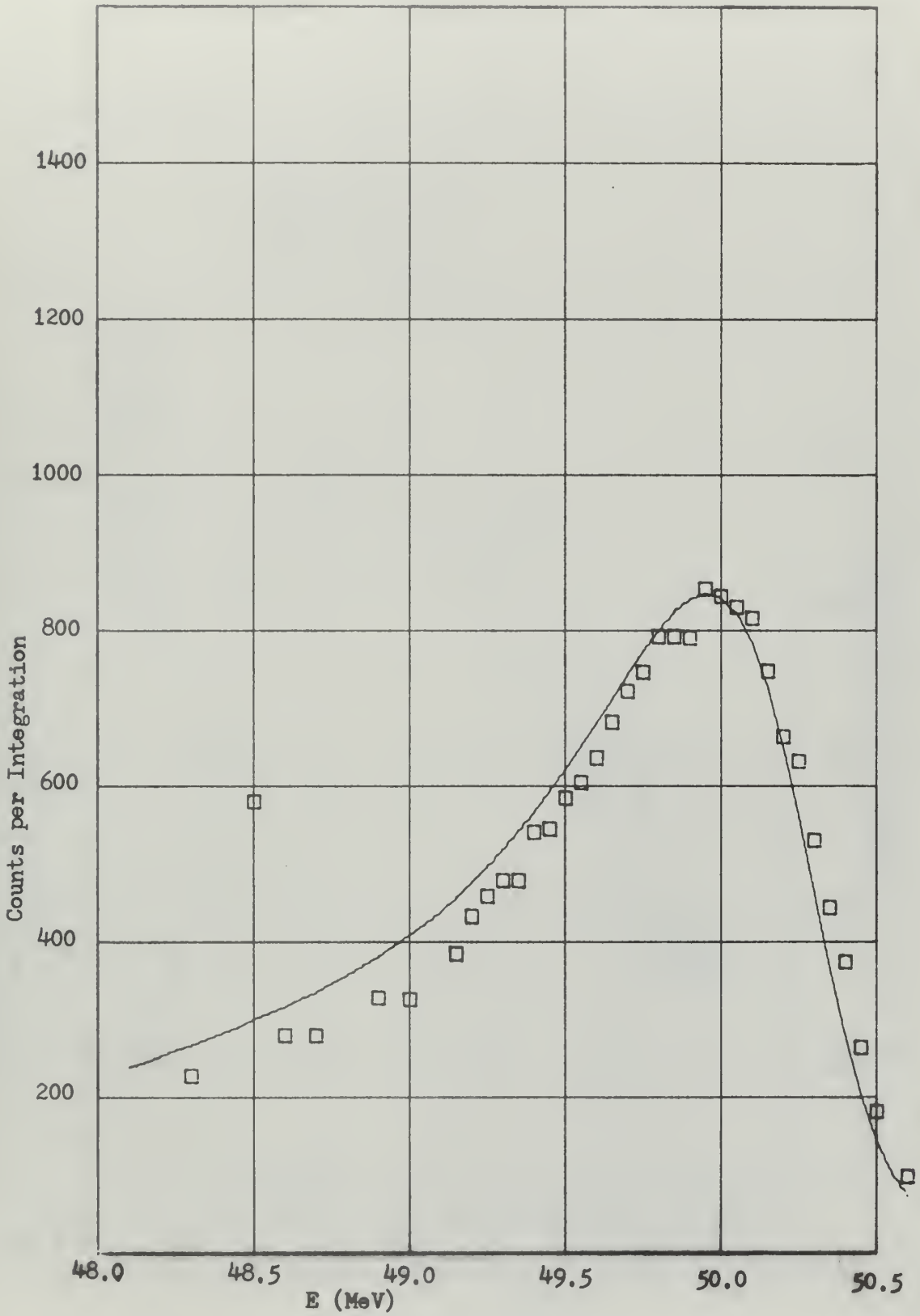


Figure 27. Predicted Distribution , Cu
t= 2.134 gm/cm$^2$ $E_i$= 52.84 MeV

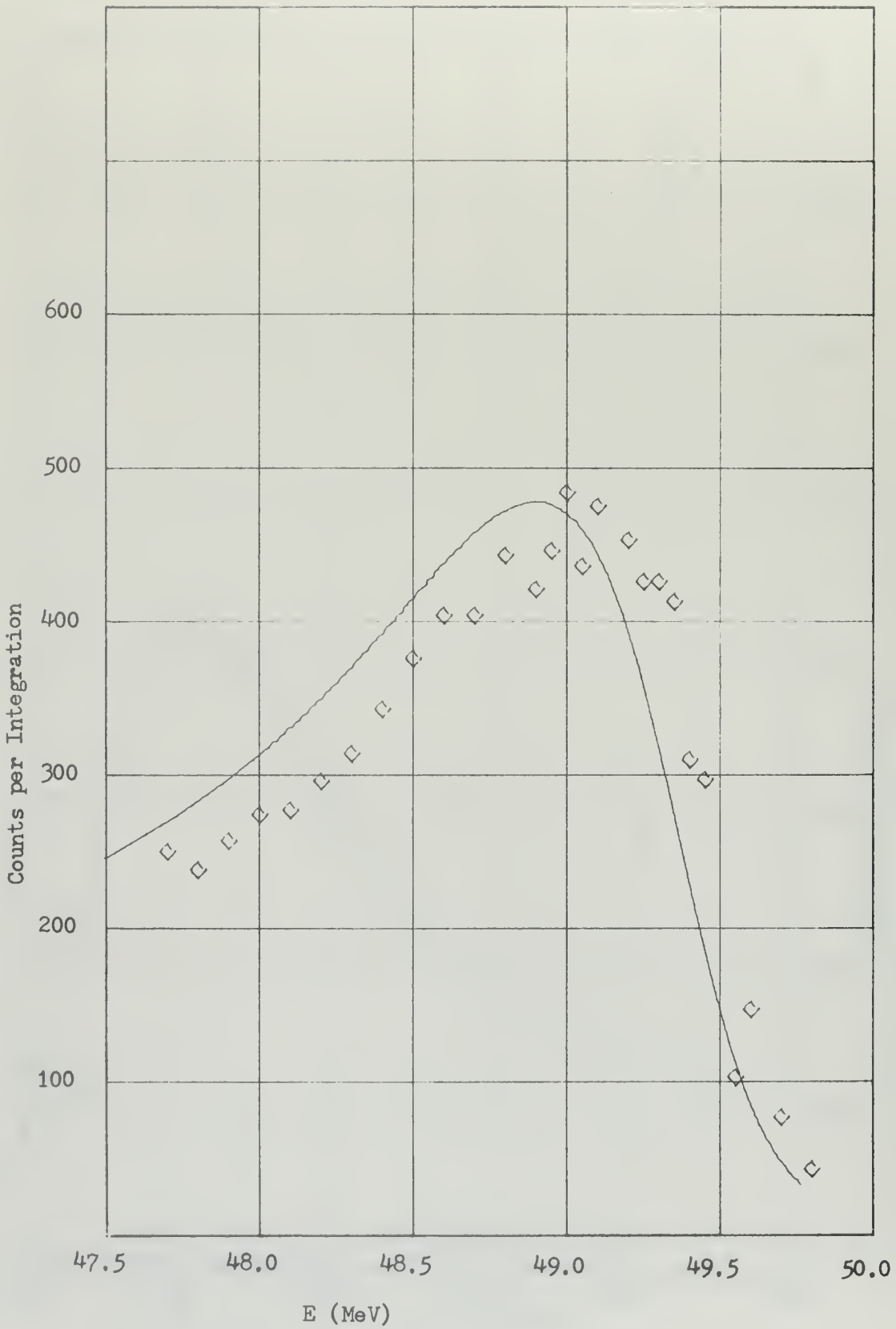


Figure 28. Predicted Distribution, Cu
$t = 2.845$ gm/cm$^2$ $E_i = 52.84$ MeV

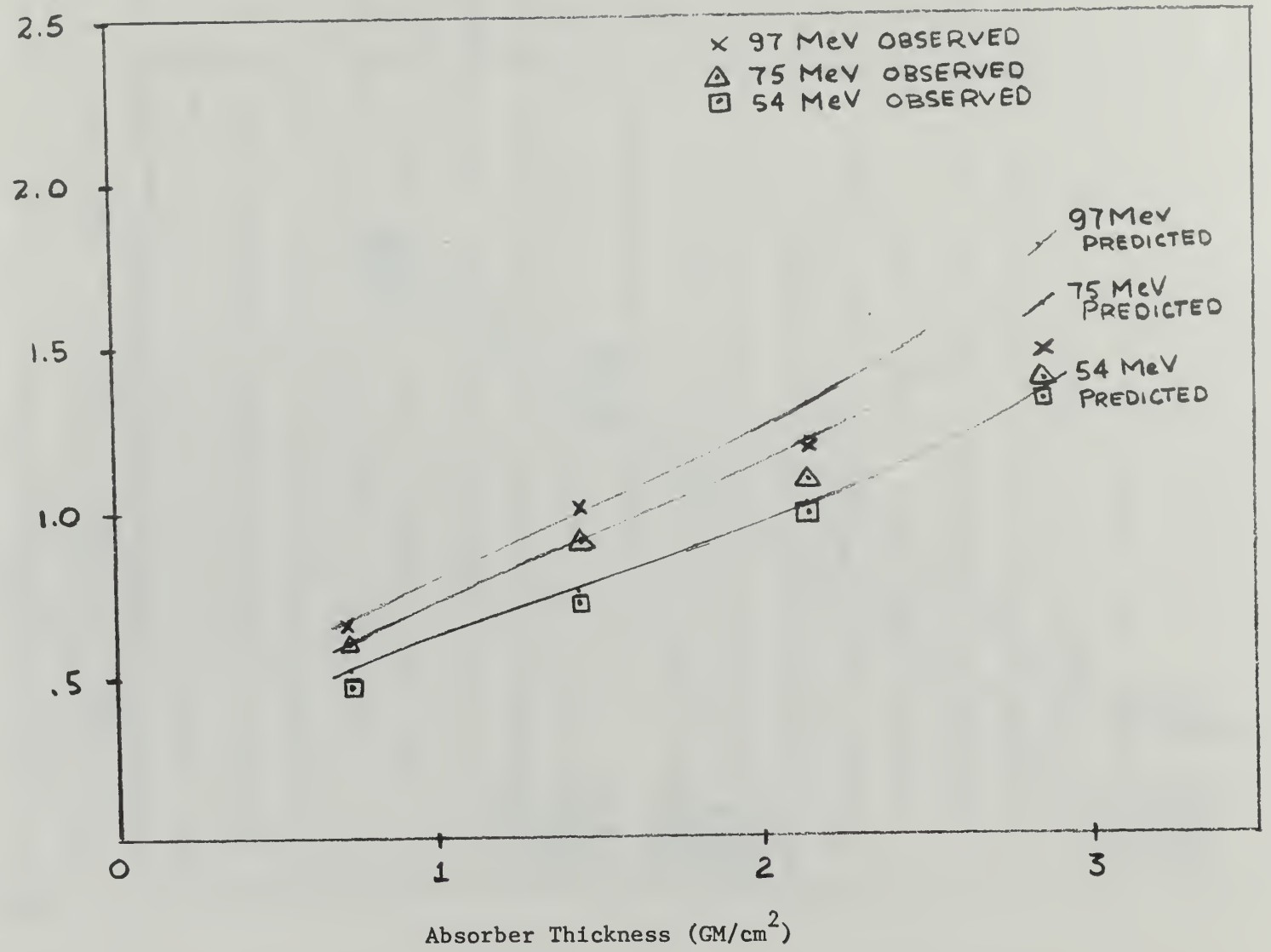


FIGURE 29. Predicted and Observed Half Widths (Aluminum)

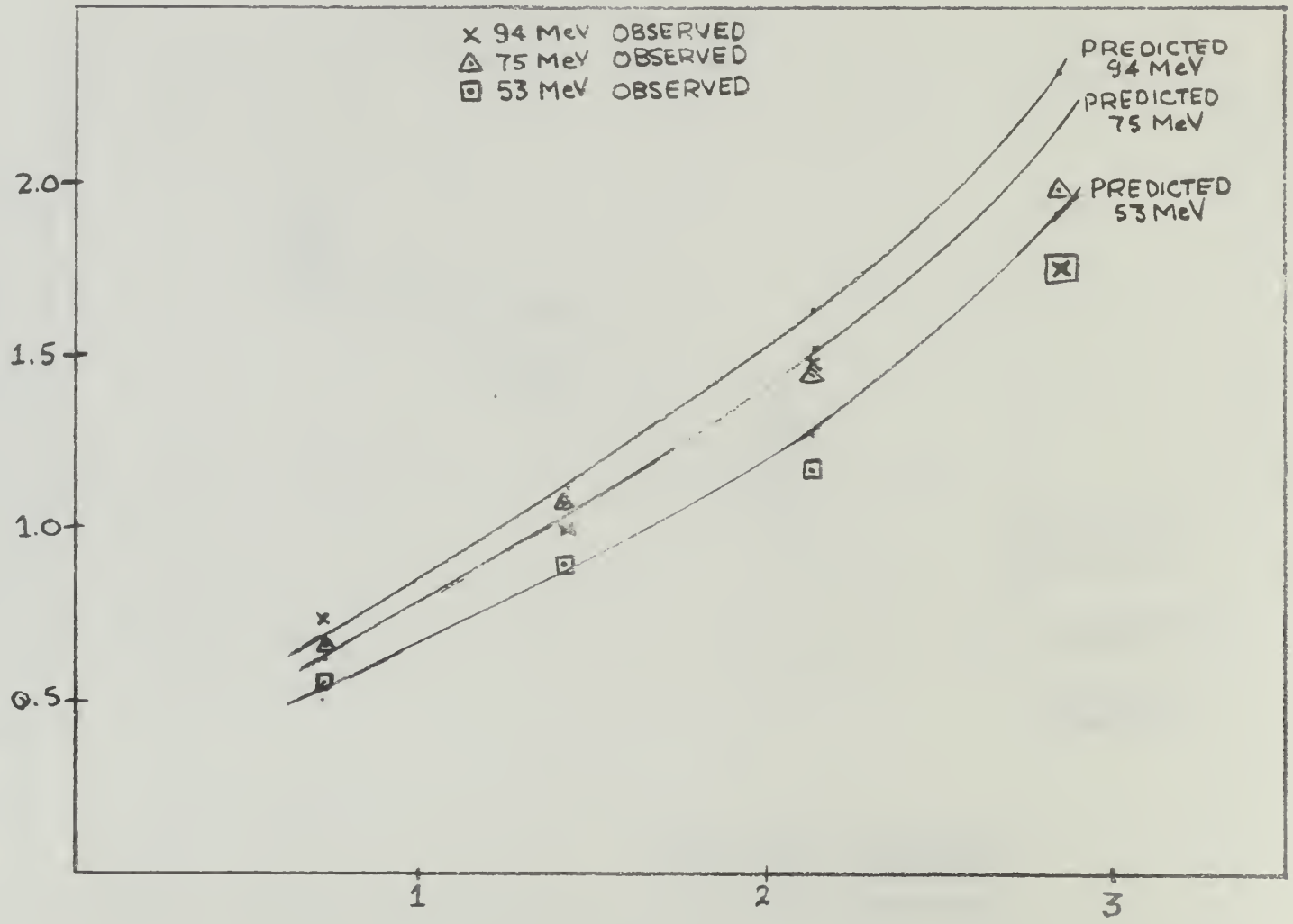


FIGURE 30. Predicted and Observed Half Widths (Copper)

## VI. DISCUSSION

An attempt was made to match absorber thicknesses and energies with Miller's work. The thinnest absorber here was to have been the same as Miller's second thinnest (0.730 versus 0.711 $gm/cm^2$); the next the same as Miller's fourth thickest (1.441 versus 1.522), etc. The differences can be explained by the inaccuracies in machining the absorbers, and the fact that a different density for aluminum was used. Miller used the tabulated value, 2.69 $gms/cm^3$. The supplier of the aluminum indicates an approximate density of 2.66 $gm/cm^3$. Weighing a sample then measuring it with a micrometer yielded 2.66, as did weighing another sample and measuring the volume of water displaced by it. Hence the value of the density of aluminum used was 2.66 $gm/cm^3$. The density of the copper samples was measured by the last two methods and found to be 8.89 $gm/cm^3$.

Generally speaking the results agree with the theory of Blunck & Westphal, indicating that both the theory and the experimental technique are good. They also agree substantially with the results obtained by Miller for energy loss. For instance Miller found at 53.7 MeV and t = 0.711 an energy loss of $1.05 \pm .07$, here we find $1.03 \pm .03$ at 53.57 MeV and t = 0.730 $gm/cm^2$. Breuer obtains approximately 1 MeV loss at 53.6 MeV with absorber thickness = 0.73 $gm/cm^2$. (He states $\Delta E_p = 1.36$ MeV/gm $cm^{-2}$) but indicates that with higher energies and thicker absorbers his experimental results diverge by increasing amounts from the theory. The conclusions to be drawn from the present results tend to confirm B & W theory and indicate that Miller is correct in his assertion that Breuer misinterpreted it.

Variation from the B & W predictions tend to be larger with thicker absorbers. Not only is the theory weaker in these regions (energy losses are larger compared to incident energy), but also the observed values are most inaccurate. The peaks are broad and not well defined. The percentage error increases as the number of counts decreases; and only by counting for a prohibitively long time can it be significantly improved; and this would be nullified to some extent by drift in the operating characteristics of the LINAC. The background is a larger fraction of the total number of counts observed, and errors made in determining the proper background are more significant. But still with all of these effects, the experiment and theory agree.

Positioning the absorber close to the scattering foil has obviated collimating the electrons leaving the absorber. This was attempted by placing a lead brick with a hole drilled in it in front of the spectrometer entrance, and the net effect was an unacceptable increase in the background with no commensurate increase in energy resolution.

Further work in this field at the NPGS LINAC is indicated, using different materials as absorbers. One would expect to find further confirmation of the B & W theory.

BIBLIOGRAPHY


1. Miller, Royce D., Energy Loss of High Energy Electrons in Aluminum, Master's Thesis, Naval Postgraduate School, (1968).

2. Yang, C. N., Physical Review, Vol. 84, page 559, (1951).

3. Rossi, B., High Energy Particles, Prentice-Hall, New York, (1952).

4. Blunck, O., and K. Westphal, Zeitschrift fur Physik, Vol 180, page 209, (1964).

5. Landau, L., Journal of Physics, USSR, Vol.8, page 201, (1944).

6. Blunck, O., and S. Leisegang, Zeitschrift fur Physik, Vol.128, page 500, (1950).

7. Eyges, L., Physical Review, Vol. 76, page 264, (1949), and Vol. 77, page 81, (1950).

8. Bethe, H., and W. Heitler, Proc. Roy. Soc., London, Series A, Vol. 146, page 83 (1934).

9. Sternheimer, R. M., (a) Physical Review, Vol. 88, page 851, (1952); (b) Physical Review, Vol. 91, page 156, (1953); (c) Physical Review, Vol. 103, page 511, (1956).

10. Hudson, A., Physical Review, Vol. 105, page 1, (1957).

11. Goldwasser, E. L., F. E. Mills, and A. O. Hanson, Physical Review, Vol. 88, page 1137,(1952).

12. Zeigler, B., Zeitschrift fur Physik, Vol. 151, page 556, (1958).

13. Breuer, H., Zeitschrift fur Physik, Vol. 180, page 209, (1964).

14. Bearden, J. A., and A. F. Burr, Reviews of Modern Physics, Vol. 19, Number 1, page 125, (January 1967).

15. Kenaston, G. W., C. T. Luke, Jr., and W. C. Sones, A Multichannel Electron Detection System for Use in a Stabilized Magnetic Spectrometer, Master's Thesis, Naval Postgraduate School, (1965).

16. Hofstadter, R., Electron Scattering and Nuclear and Nucleon Structure, W. A. Benjamin, Inc., New York, (1963); paper number 42.

17. Tables of Energy Losses and Ranges of Electrons and Positrons. Berger and Seltzer, NASA Publication SP-3012, (1964).

18. Browman, A., Ph. D. dissertation, Stanford University, 1964, (unpublished).

19. Oberdier, Lyn D., The Optical Performance of the 16 Inch Magnetic Spectrometer, Master's Thesis, Naval Postgraduate School, (1967).

APPENDIX A. Derivation of Expression for Recoil Energy. ($90^{o}$ scattering).

$E_e$ = Incident electron energy

$E_e'$ = final electron energy

M = rest mass of the struck nucleus

$E_a$ = final energy of the struck nucleus

From conservation of mass and momentum:

$$E_e + M = E_e' + E_a \quad \text{and} \quad p^2 = p_e^{\,2} + p_e'^{\,2}$$

from these we find:

$$E_e' = (E_e + M - E_a)$$

$$E_e'^{\,2} = (E_e + M - E_a)^2$$

$$E_e'^{\,2} = (E_e^{\,2} + M^2 + E_a^{\,2} + 2E_eM - 2E_aM - 2E_eE_a)$$

The term $E_a^{\,2}$ will be neglected because it is second order in $E_a$, which is small compared to $E_e$ and M.

$$E_e'^{\,2} = E_e^{\,2} + M^2 + 2E_eM - 2E_aM - 2E_eE_a.$$

Similarly p is small compared to $p_e$ and $p_e'$ so we neglect $p^2$.

$$p_e'^{\,2} = p_e^{\,2}$$

$$m^2 = M^2 + p_e^{\,2} + E_e'^{\,2}$$

$$m^2 = M^2 + p_e^{\,2} + E_e^{\,2} + M^2 + 2E_eM - 2E_a(M - E_e)$$

from which

$$E_a = \frac{M^2 + p_e^{\,2} + E_e^{\,2} + M^2 + 2E_eM}{2(M + E_e)}$$

$$T_a = \frac{2M^2 + p_e^{\,2} + E_e^{\,2} + 2E_eM}{2(M + E_e)} - M$$

$$T_a = \frac{2M^2 + p_e^2 + E_e^2 + 2E_eM - 2M^2 - 2E_eM}{2(M + E_e)}$$

$$T_a = \frac{p_e^2 + E_e^2}{2(M + E_e)} = \frac{p_e^2 + p_e^2 + m^2}{2(M + E_e)} = \frac{2p_e^2 + m^2}{2(M + E_e)}$$

here $m^2$ is small compared to the other terms.

$$T_a = \frac{p_e^2}{(M + E_e)}$$ (within approximations noted).

APPENDIX B. Computer Program for Counting Rate Corrections
(Miller's method)

```
C     PROGRAM TO CORRECT COUNTING DATA FOR HIGH COUNTING RATE.
      DIMENSION E(150),EN(6,150),T(6,150),N(6,150),ZUM(6),BKGD(6)
      READ (5,99) M
   99 FORMAT (I3)
      READ (5,100) (E(J),EN(1,J),T(1,J),EN(2,J),T(2,J),EN(3,J),T(3,J),
     1  EN(4,J),T(4,J),EN(5,J),T(5,J),EN(6,J),T(6,J), J=1,M)
  100 FORMAT (13F5.0)
      READ(5,101) BKNR,(ZUM(I),I=1,6),FACT
  101 FORMAT (8F5.0)
C     ZUM IS A FACTOR TO ADJUST THE BACKGROUND TO COMPENSATE FOR DIFFERE
C     CHARGE INTEGRATIONS WITH DIFFERENT ABSORBERS.
      DO 200 J=1,M
      DO 201 I=1,6
      BKGD(I)=ZUM(I)*BKNR
  201 N(I,J)=EN(I,J)/(1.-((FACT*EN(I,J))/(1000.*T(I,J)+.0000001)))
     1-BKGD(I)
  200 CONTINUE
      WRITE (6,400)
  400 FORMAT (1H1, 72HENERGY                0           1           2
     1          3
     2          4          5          6)
      WRITE (6,300) (E(J),N(1,J),N(2,J),N(3,J),N(4,J),N(5,J),N(6,J),
     1  J=1,M)
  300 FORMAT (F10.3,6I10)
      DO 90 LK=1,6
      DO 80 LS=1,M
   80 WRITE(7,900)  E(LS),N(LK,LS)
   90 CONTINUE
  900 FORMAT(' ',F7.3,6X,I5)
      STOP
      END
```

Appendix C. Computer Program for Counting Rate Corrections
(rate less than 6 counts per second).

```
C       PROGRAM TO CORRECT COUNTING DATA FOR HIGH COUNTING RATE.
        DIMENSION E(150),EN(6,150),T(6,150),N(6,150),ZUM(6),BKGD(6),CMP(6
       1,150),CMPC(6,150)
        READ (5,99) M
     99 FORMAT (I3)
        READ (5,100) (E(J),EN(1,J),T(1,J),EN(2,J),T(2,J),EN(3,J),T(3,J),
       1 EN(4,J),T(4,J),EN(5,J),T(5,J),EN(6,J),T(6,J), J=1,M)
    100 FORMAT (13F5.0)
        READ(5,101) BKNR,(ZUM(I),I=1,6),FACT
    101 FORMAT (8F5.0)
C       ZUM IS A FACTOR TO ADJUST THE BACKGROUND TO COMPENSATE FOR DIFFERE
C       CHARGE INTEGRATIONS WITH DIFFERENT ABSORBERS.
        DO 200 J=1,M
        DO 201 I=1,6
        BKGD(I)=ZUM(I)*BKNR
        CMP(I,J)=EN(I,J)/((T(I,J)*60.)+.0000001)
        CMPC(I,J)=CMP(I,J)*(1.+.6*CMP(I,J))
    201 N(I,J)=(CMPC(I,J)*60.*T(I,J))-BKGD(I)
C       CMP IS COUNTS PER MACHINE PULSE, CMPC IS A CORRECTED CMP, 60 IS
C       FROM 60 MACHINE PULSES PER SECOND.
    200 CONTINUE
        WRITE (6,400)
    400 FORMAT (1H1, 72HENERGY                0                1
       1        2        3
       2        4        5        6//)
        WRITE (6,300) (J),N(1,J),N(2,J),N(3,J),N(4,J),N(5,J),N(6,J),
       1 J=1,M)
    300 FORMAT (F10.3,6I10)
        DO 90 LK=1,6
        DO 80 LS=1,M
     80 WRITE(7,900)   E(LS),N(LK,LS)
     90 CONTINUE
    900 FORMAT('  ',F7.3,6X,I5)
        STOP
        END
```

APPENDIX D. Computer Program for Computing Various Distribution Parameters (Aluminum).

```
C     PROGRAM TO CALCULATE VARIOUS DISTRIBUTION PARAMETERS AND RELATED
C     QUANTITIES  FOR ALUMINUM
      DIMENSION   DELEP(5,8), EIN(5),  T(8)
      DIMENSION   QBAR(5,8)
      DIMENSION   B2(5,8),QZERO(5,8),A(5,8)
      DIMENSION   DELEPG(5,8)
      DIMENSION   ALFR(5,8)
      READ (5,104) (T(J), J=1,8)
  104 FORMAT (8F8.4)
      READ (5,102)  (EIN(I),  I=1,5)
  102 FORMAT (5F10.2)
      WRITE (6,299)
  299 FORMAT (1H1, 9HTHICKNESS,30X 20HPROBABLE ENERGY LOSS/ 1H ,
     1  7HGM/CMSQ ,45X, 3HMEV)
      WRITE (6,105) (EIN)
  105 FORMAT (1H0,11X, 5(5X,F7.2)//)
      DO 201 J=1,8
      DO 200 I=1,5
      BSQ = (EIN(I)**2+1.022*EIN(I))/((EIN(I)+0.511)**2)
      DELEP(I,J)=(0.0740*T(J)/BSQ)*(22.04+ALOG((0.0740*T(J))/BSQ)-BSQ-
     10.0906*((3.0-ALOG10(SQRT(EIN(I)**2+1.022*EIN(I))/.511))**3.511))
      DELEPG(I,J)=DELEP(I,J)/T(J)
      QBAR(I,J) =(0.0740*T(J)/BSQ)*(21.41+ALOG(EIN(I))-BSQ-
     10.0906*((3.0-ALOG10(SQRT(EIN(I)**2+1.022*EIN(I))/.511))**3.511))
      A(I,J)=0.154*13.0*T(J)/(26.97*BSQ)
      G=2.0*EIN(I)*(EIN(I)+0.511)*(EIN(I)+0.511)/(0.511*0.511)
      B2(I,J)=(3.00/13.0/A(I,J))*(0.0034*ALOG(  G/0.0017)+0.000065*6.0*
     1 ALOG(   G/0.000065)+0.000100*ALOG(   G/0.000020) )
      QZERO(I,J)=QBAR (I,J)+A(I,J)*(1.116-ALOG(EIN(I)/A(I,J)) )
      ALFR(I,J)=T(J)*0.0014*13.0*13.0/26.97*(1.333*ALOG(183.0/(13.0**(1
     1./3.)))+1.0/9.0
  200 CONTINUE
  201 CONTINUE
      WRITE (6, 300) (T(J),DELEP(1,J), DELEP(2,J),  DELEP(3,J), DELEP(
     14,J),J=1,8)
  300 FORMAT (6H DELEP(5,J), J=1,8)
      WRITE (6,301)
      WRITE (6,300) (T(J),DELEPG(1,J),DELEPG(2,J),DELEPG(3,J),DELEPG(4,J
     1),DELEPG(5,J),  J=1,8)
  301 FORMAT (6H QBAR(5,J), J=1,8)
      WRITE (6,301)
      WRITE (6,300)  (T(J),QBAR(1,J),QBAR(2,J),QBAR(3,J),QBAR(4,J),
     1 QBAR(5,J),J=1,8)
      WRITE (6,301)
      WRITE (6,300)  (T(J),QZERO(1,J),QZERO(2,J),QZERO(3,J),QZERO(4,J),
     1 QZERO(5,J),J=1,8)
      WRITE (6,301)
```

APPENDIX E. Computer Program for Computing Various Distribution Parameters (Copper).

```
      WRITE (6,300) (T(J),B2(1,J),B2(2,J),B2(3,J),B2(4,J),B2(5,J),J=1,
     1   8)
          WRITE (6,301)
          WRITE (6,300) (T(J),A(1,J),A(2,J),A(3,J),A(4,J),A(5,J), J=1,8)
          WRITE (6,301)
          WRITE (6,300) (T(J),ALFR(1,J),ALFR(2,J),ALFR(3,J),ALFR(4,J),
     1 ALFR(5,J),J=1,8)
  300 FORMAT (6(5X, F7.5))
  301 STOP
      END
C     ------------------------------------------------------------------
C     FIRST DATA CARD 8 THICKNESSES OF ABSORBERS  IN REQUIRED FORMAT.
C     SECOND DATA CARD 5 INITIAL ENERGY VALUES IN REQUIRED FORMAT.
C
C
C     PROGRAM TO CALCULATE VARIOUS DISTRIBUTION PARAMETERS AND RELATED
C     QUANTITIES FOR COPPER.
      DIMENSION DELEP(5,8), EIN(5),  T(8)
      DIMENSION QBAR(5,8)
      DIMENSION B2(5,8),QZERO(5,8),A(5,8)
      DIMENSION DELEPG(5,8)
      DIMENSION ALFR(5,8)
      READ (5,104) (T(J), J=1,8)
  104 FORMAT (8F8.4)
      READ (5,102) (EIN(I),  I=1,5)
  102 FORMAT (5F10.2)
      WRITE (6,299)
  299 FORMAT (1H1, 9HTHICKNESS,30X 20HPROBABLE ENERGY LOSS/ 1H ,
     1  7HGM/CMSQ ,45X, 3HMEV)
      WRITE (6,105) (EIN)
  105 FORMAT (1HO,11X, 5(5X,F7.2)//)
      DO 200 J=1,8
      BSQ = (EIN(I)**2+1.022*EIN(I))/((EIN(I)+0.511)**2)
      DELEP(I,J)=(0.0701*T(J)/BSQ)*(20.89+ALOG((0.0701*T(J))/BSQ)-BSQ-
     10.119*((3.0-ALOG10(SQRT(EIN(I)**2+1.022*EIN(I))/.511))**3.38))
      DELEPG(I,J)=DELEP(I,J)/T(J)
      QBAR(I,J)=(0.0701*T(J)/BSQ)*(20.26+ALOG(EIN(I))-BSQ-0.119*((3.0-
     1ALOG10(SQRT(EIN(I)**2+1.022*EIN(I))/.511))**3.38))
        A(I,J)=0.154*29.0*T(J)/(63.54*BSQ)
        G=2.0*EIN(I)*(EIN(I)+0.511)*(EIN(I)+0.511)/(0.511*0.511)
```

```
      B2(I,J)=(2.60/29.0/A(I,J))*(.018006*ALOG(G/.009003)+0.00098*6.*
     1ALOG(G/0.00098) .000073*10.*ALOG(G/.000073)+0.000008*11.*ALOG(G/
     10.000008))
      QZERO(I,J)=QBAR (I,J)+A(I,J)*(1.116-ALOG(EIN(I)/A(I,J)) )
      ALFR(I,J)=T(J)*0.0014*29.0*29.0/63.54*((4./3.)*ALOG(183./(29.**(
     11./3.)))+1./9.)
  200 CONTINUE
  201 CONTINUE
      WRITE (6, 300) (T(J),DELEP(1,J), DELEP(2,J),  DELEP(3,J), DELEP(
     14,J), DELEP(5,J), J=1,8)
      WRITE (6,301)
      WRITE (6, 300)(T(J),DELEPG(1,J),DELEPG(2,J),DELEPG(3,J),DELEPG(4,J
     1),DELEPG(5,J),  J=1,8)
      WRITE (6,301)
      WRITE (6,300) (T(J),QBAR(1,J),QBAR(2,J),QBAR(3,J),QBAR(4,J),
     1 QBAR(5,J),  J=1,8)
      WRITE (6 ,301)
      WRITE (6,300) (T(J),QZERO(1,J),QZERO(2,J),QZERO(3,J),QZERO(4,J),
     1 QZERO(5,J),  J=1,8)
      WRITE (6,301)
      WRITE (6,300) (T(J),B2(1,J),B2(2,J),B2(3,J),B2(4,J),B2(5,J),J=1,
     1   8)
      WRITE (6,301)
      WRITE  (6,300) (T(J),A(1,J),A(2,J),A(3,J),A(4,J),A(5,J), J=1,8)
      WRITE (6,301)
      WRITE (6,300)  (T(J),ALFR(1,J),ALFR(2,J),ALFR(3,J),ALFR(4,J),
     1 ALFR(5,J), J=1,8)
  300 FORMAT (6(5X, F7.5))
  301 FORMAT (1H0/)
      STOP
      END
```

APPENDIX F. Computer Program for Distribution Calculations

```
      DIMENSION FEF(400),FEI(300),FQQ(100),EF(400)
      READ (5,20) AMP
      READ (5,20) AMPX
   2C FORMAT (F5.0)
      READ (5,400) N
      READ (5,400) M
  40C FORMAT (I3)
      READ (5,399) (EIS, A, QZERO, C)
  399 FORMAT (4F10.0)
      READ (5,401) (FQQ(I),I=1,N)
      READ (5,401) (FEI(I), I=1,M)
  401 FORMAT (F10.0)
      DO 499 K=1,400
  499 FEF(K)=0.0000000000000000
      DO 700 J=1,N
      DO 700 I=1,M
  700 FEF(I+J-1)=FEF(I+J-1)+FQQ(J)*FEI(I)*AMP
  701 CONTINUE
      LP=N+M-1
      DQ=FEF(1)
      DO 710 I=1,LP
      IF(DQ.LT.FEF(I))DQ=FEF(I)
  710 CONTINUE
      AMF=AMPX/DQ*1000.
      DO 75 K=1,400
   75 FEF(K)=0.0000000000000000
      DO 501 J=1,N
      DO 500 I=1,M
      FEF(I+J-1)=FEF(I+J-1)+FQQ(J)*FEI(I)*AMP
      B=(I+J-1)
      EF(I+J-1)=EIS-QZERO+5.0*A-B*A/C
      L=M+N-1
  500 CONTINUE
  501 CONTINUE
      WRITE (6,600) (EF(I), FEF(I), I=1,L)
  600 FORMAT (1H1, 18H  ENERGY      COUNT // (F10.6, F10.4))
      DO 80 LS=1,L
   80 WRITE(7,900) EF(LS),FEF(LS)
  90C FORMAT(1X,F7.3,6X,F5.0)
      STOP
      END
```

INITIAL DISTRIBUTION LIST

| | | No. Copies |
|---|---|---|
| 1. | Defense Documentation Center<br>Cameron Station<br>Alexandria, Virginia 22314 | 20 |
| 2. | Library<br>Naval Postgraduate School<br>Monterey, California 93940 | 2 |
| 3. | Office of Naval Research<br>Washington, D. C. | 1 |
| 4. | Professor Fred R. Buskirk<br>Department of Physics<br>Naval Postgraduate School<br>Monterey, California 93940 | 20 |
| 5. | Major Royce D. Miller, USA<br>Mathematics Department<br>U. S. Military Academy<br>West Point, New York | 1 |
| 6. | LCDR J. C. Goodwin, Jr., USN<br>1610 Canterbury Road<br>Raleigh, North Carolina 27608 | 2 |

## DOCUMENT CONTROL DATA - R & D

*(Security classification of title, body of abstract and indexing annotation must be entered when the overall report is classified)*

1. ORIGINATING ACTIVITY *(Corporate author)*
Naval Postgraduate School
Monterey, California 93940

2a. REPORT SECURITY CLASSIFICATION
Unclassified

2b. GROUP

3. REPORT TITLE

Energy Loss of High Energy Electrons in Aluminum and Copper

4. DESCRIPTIVE NOTES *(Type of report and, inclusive dates)*
Master of Science Thesis, December 1968

5. AUTHOR(S) *(First name, middle initial, last name)*
James C. Goodwin, Jr.

| 6. REPORT DATE | 7a. TOTAL NO. OF PAGES | 7b. NO. OF REFS |
|---|---|---|
| December 1968 | 73 | 19 |

| 8a. CONTRACT OR GRANT NO. | 9a. ORIGINATOR'S REPORT NUMBER(S) |
|---|---|
| N/A | N/A |
| b. PROJECT NO. N/A | |
| c. | 9b. OTHER REPORT NO(S) *(Any other numbers that may be assigned this report)* |
| d. N/A | N/A |

10. DISTRIBUTION STATEMENT

This document has been approved for public release and sale; its distribution is unlimited.

| 11. SUPPLEMENTARY NOTES | 12. SPONSORING MILITARY ACTIVITY |
|---|---|
| N/A | Naval Postgraduate School<br>Monterey, California 93940 |

13. ABSTRACT

The LINAC at NPGS, Monterey was used to accelerate electrons to energies ranging from 50 - 100 MeV. These were used to study energy losses of high energy electrons in aluminum and copper. The densities of each material ranged from 0.7 to 2.8 gm/cm$^2$.

The results agreed with the theory of Blunck and Westphal, unlike previous measurements made by Breuer who found disagreement between his experimental results and his interpretation of the theory of Blunck and Westphal, particularly at energies above 50 MeV and with aluminum of thickness greater than that yielding a density of 1 gm/cm$^2$.

| 14. KEY WORDS | LINK A | | LINK B | | LINK C | |
|---|---|---|---|---|---|---|
| | ROLE | WT | ROLE | WT | ROLE | WT |
| Electrons, Energy Loss of in Aluminum and Copper | | | | | | |
| Energy Loss, of Electrons in Aluminum and Copper | | | | | | |
| Aluminum, Energy Loss of Electrons in | | | | | | |
| Copper, Energy Loss of Electrons in | | | | | | |